Flavor physics in SU(5) GUT with scalar fields in the 45 representation

Toru Goto,[1] Satoshi Mishima,[1,2] and Tetsuo Shindou[3]

[1]*Theory Center, IPNS, KEK, Tsukuba 305-0801, Japan*

[2]*Department of Liberal Arts, Saitama Medical University, Moroyama, Saitama 350-0495, Japan*

[3]*Division of Liberal-Arts, Kogakuin University, 2665-1 Nakano-machi, Hachioji, Tokyo 192-0015, Japan*

(Received 6 September 2023; accepted 4 October 2023; published 7 November 2023)

We study a realistic SU(5) grand unified model, where a **45** representation of scalar fields is added to the Georgi-Glashow model in order to realize the gauge coupling unification and the masses and mixing of quarks and leptons. The gauge coupling unification together with constraints from proton decay implies mass splittings in scalar representations. We assume that an SU(2) triplet component of the **45** scalar, which is called S_3 leptoquark, has a TeV-scale mass, and color-sextet and color-octet ones have masses of the order of 10^6 GeV. We calculate one-loop beta functions for Yukawa couplings in the model, and derive the low-energy values of the S_3 Yukawa couplings which are consistent with the grand unification. We provide predictions for lepton-flavor violation and lepton-flavor-universality violation induced by the S_3 leptoquark, and find that current and future experiments have a chance to find a footprint of our SU(5) model.

DOI: 10.1103/PhysRevD.108.095012

I. INTRODUCTION

The idea of Grand Unification is an attractive candidate for the fundamental theory behind the present understanding of particle physics described by the Standard Model (SM) [1–6]. Although the SM has been established as a successful effective model at the electroweak (EW) scale by the discovery of the Higgs boson, reaching a deeper understanding of nature is a desire of particle physicists. Interestingly, some properties of the SM suggest the existence of a Grand Unified Theory (GUT) as a high-energy theory beyond the SM. For example, the renormalization group (RG) runnings of the gauge couplings in the SM show a unification tendency at a high scale [4], and the charge quantization of the SM fermions suggests the unification of matter. Once the SM gauge groups for electromagnetic, weak, and strong interactions are unified to a GUT gauge symmetry group, quarks and leptons are consequently unified in a single or a few representations of the GUT group. Various groups, such as SU(5), SO(10), E_6, etc., have been considered as the GUT gauge symmetry group [7].

The SU(5) is the minimal simple group which contains the SM gauge groups $SU(3)_C \times SU(2)_L \times U(1)_Y$. The minimal version of the GUT model based on the SU(5) symmetry, called the minimal SU(5) GUT, was originally proposed by Georgi and Glashow [3]. In the minimal SU(5) GUT model, the right-handed down quarks and the left-handed lepton doublets are embedded in $\bar{\mathbf{5}}$ representations of SU(5), and the left-handed quark doublets, the right-handed up quarks, and the right-handed charged leptons are embedded in **10** representations. The SM Higgs doublet is embedded in a **5** representation of scalars. In addition, the minimal model also contains a **24** representation of scalars, which breaks the SU(5) gauge symmetry to the SM ones.

Although the concept of the minimal SU(5) GUT is beautiful, there are two serious issues that have to be solved to construct a more realistic model. First, the three gauge couplings are not unified at a high-energy scale only with the RG runnings in the SM. In the minimal SU(5) model, there is a grand desert between the EW and the GUT scales, where there is no new contribution to the RG runnings. Second, the measured values of the masses of the charged leptons and the down-type quarks cannot be accommodated with the minimal SU(5) GUT, where they originate from a common Yukawa interaction in the GUT Lagrangian.

The first issue on the gauge coupling unification can be overcome by introducing extra fields in the grand desert, since such fields modify the RG runnings of the gauge couplings. A famous example of this direction is the supersymmetric SU(5) GUT model, in which the superpartners of the SM particles as well as the second Higgs doublet are introduced and the gauge coupling unification occurs at the scale of the order of 10^{16} GeV [8–12]. In nonsupersymmetric SU(5) GUT models, a single or a few particles in an extra representation of SU(5) are predicted to lie in the grand desert in order to realize the gauge coupling unification [13–30].

The second issue on the masses of the charged leptons and the down-type quarks can be resolved by introducing a **45** representation of scalar fields to the minimal SU(5) GUT. Similar to the **5** scalar, the **45** scalar couples with the **10** and the $\bar{\mathbf{5}}$ fermions since $\mathbf{10}\otimes\bar{\mathbf{5}}=\mathbf{5}\oplus\mathbf{45}$. This coupling makes modifications in the relation between the charged-lepton and the down-type-quark Yukawa matrices at the GUT scale through the Georgi-Jarlskog mechanism [31].

We combine the above two ideas on the extensions of the minimal SU(5) GUT, and construct a concrete example of a realistic SU(5) GUT model, where the gauge coupling unification and the correct fermion masses are realized simultaneously. This kind of model having the **45** scalar can be found, for example, in Refs. [13,15,18,21–25,27,28]. In the current study, we introduce the **45** scalar to reproduce the charged-lepton and the down-type-quark Yukawa matrices correctly, and make an SU(2) triplet component of the **45** scalar light enough to achieve the gauge coupling unification [18]. This triplet scalar is called S_3^*. The Yukawa interactions between the **45** scalar and the **10** and the $\bar{\mathbf{5}}$ fermions are given by $\mathbf{10}\cdot\mathbf{10}\cdot\mathbf{45}$ and $\mathbf{10}\cdot\bar{\mathbf{5}}\cdot\overline{\mathbf{45}}$, where we omit the former by hand to suppress baryon-number-violating interactions mediated by the light S_3^*. In addition to the S_3^*, we assume that color-sextet and color-octet components in the **24** and the **45** scalars have masses of the order of 10^6 GeV in order to avoid too rapid proton decay mediated by the GUT gauge bosons.[1] In this case, the SU(2) triplet scalar has a mass of $\mathcal{O}(10^3$–10^6 GeV), and the GUT scale is of $\mathcal{O}(10^{16}$–10^{17} GeV). We do not consider any mechanisms to generate the mass splittings in the GUT multiplets and to forbid the $\mathbf{10}\cdot\mathbf{10}\cdot\mathbf{45}$ interactions, which are beyond the scope of the current work. Moreover, we do not specify the origin of the nonzero neutrino masses, which are studied in the framework of the SU(5) GUT with the **45** scalar, for example, in Refs. [21,22,25,27,32–34].

This triplet scalar S_3^* carries the SM gauge quantum numbers $(\mathbf{3},\mathbf{3},-1/3)$, and has Yukawa couplings to a lepton and a quark. The conjugate state of S_3^*, having $(\bar{\mathbf{3}},\mathbf{3},1/3)$, is often called S_3 leptoquark [35,36]. If the mass of the S_3 leptoquark lies at the TeV scale, S_3 can affect various flavor observables. Unlike the phenomenological models where the S_3 leptoquark is introduced by hand as, for instance, in Refs. [37–48], the flavor structure of the Yukawa couplings associated with S_3 is constrained by the measured values of the charged-lepton and the down-type quark masses. It provides peculiar correlations in the flavor observables. We study the impact of the S_3 leptoquark at the TeV scale in our model on the phenomenology of flavor observables, such as leptonic and semileptonic B decays, $B_s-\bar{B}_s$ mixing, $\Upsilon(nS)$ decays, tau-lepton decays, and $Z\to\mu^{\mp}\tau^{\pm}$ decay. We show that Belle II with 50 ab^{-1} and LHCb with 300 fb^{-1} have a chance to find a footprint of our SU(5) GUT model.

This paper is organized as follows. In Sec. II, we introduce an SU(5) GUT model with a **45** scalar, and explain how it solves the issues in the minimal SU(5) GUT. In Sec. III, we present and discuss phenomenological implications of our model. Section IV contains our summary and conclusions. Some technical details are given in the Appendixes.

II. MODEL

A. Lagrangian

We consider an SU(5) GUT model, where the SM fermions reside in **10** and $\bar{\mathbf{5}}$ representations of SU(5), denoted by Ψ_{10i} and $\Psi_{\bar{5}i}$ with $i=1,2,3$ being the generation index, and the scalar sector is composed of one **24**, one **5**, and one **45**-dimensional scalar representation, denoted by Σ, Φ_5, and Φ_{45}, respectively. The SU(5)-symmetric renormalizable Lagrangian is given by

$$\begin{aligned}\mathcal{L}=&-\frac{1}{4}(V^{\mu\nu})^B{}_A(V_{\mu\nu})^A{}_B+i(\bar{\Psi}_{10i})_{AB}\gamma^\mu D_\mu(\Psi_{10i})^{AB}\\&+i(\bar{\Psi}_{\bar{5}i})^A\gamma^\mu D_\mu(\Psi_{\bar{5}i})_A+[D^\mu\Sigma^B{}_A][D_\mu\Sigma^A{}_B]\\&+[D^\mu(\Phi_5^\dagger)_A][D_\mu(\Phi_5)^A]+[D^\mu(\Phi_{45}^\dagger)^C_{AB}][D_\mu(\Phi_{45})^{AB}_C]\\&+\mathcal{L}_Y-V(\Sigma,\Phi_5,\Phi_{45}),\end{aligned}\tag{1}$$

where $V_{\mu\nu}$ is the field strength tensor of the SU(5) gauge bosons, $A,B,C=1,\ldots,5$ are SU(5) indices, and $\mathcal{L}_Y$ and $V(\Sigma,\Phi_5,\Phi_{45})$ represent the Yukawa interactions and the scalar potential, respectively. The summation over repeated indices is implied. Here the fields Ψ_{10i}, Σ, and Φ_{45} satisfy the following relations:

$$\begin{aligned}&(\Psi_{10i})^{AB}=-(\Psi_{10i})^{BA},\qquad(\Sigma^B{}_A)^*=\Sigma^A{}_B,\qquad\Sigma^A{}_A=0,\\&(\Phi_{45})^{AB}_C=-(\Phi_{45})^{BA}_C,\qquad(\Phi_{45})^{AB}_A=0.\end{aligned}\tag{2}$$

In general the Yukawa term $\mathcal{L}_Y$ in Eq. (1) consists of the four interactions:

$$\begin{aligned}-\mathcal{L}_Y=&\frac{1}{8}(Y_5^U)_{ij}\epsilon_{ABCDE}(\Psi_{10i})^{AB}(\Phi_5)^C(\Psi_{10j})^{\mathrm{DE}}\\&+(Y_5^D)_{ij}(\Psi_{10i})^{AB}(\Phi_5^\dagger)_A(\Psi_{\bar{5}j})_B\\&+\frac{1}{4}(Y_{45}^U)_{ij}\epsilon_{ABCDE}(\Psi_{10i})^{AB}(\Phi_{45})^{CD}_F(\Psi_{10j})^{EF}\\&+\frac{1}{2}(Y_{45}^D)_{ij}(\Psi_{10i})^{AB}(\Phi_{45}^\dagger)^C_{AB}(\Psi_{\bar{5}j})_C+\mathrm{H.c.},\end{aligned}\tag{3}$$

[1]For example, one can increase the GUT scale to evade the constraint from the proton decay by making the $(\mathbf{8},\mathbf{2},1/2)$ scalar in the **45** representation light [13,18,30].

where the totally antisymmetric tensor is defined as $\epsilon_{12345} = 1$, and Y_5^U and Y_{45}^U are symmetric and antisymmetric matrices in the generation space, respectively:

$$(Y_5^U)_{ij} = (Y_5^U)_{ji}, \qquad (Y_{45}^U)_{ij} = -(Y_{45}^U)_{ji}. \tag{4}$$

The explicit expression for the scalar potential $V(\Sigma, \Phi_5, \Phi_{45})$ is given in Appendix A.

The SU(5) gauge symmetry is assumed to be broken down to the SM gauge symmetry $\mathrm{SU}(3)_\mathrm{C} \times \mathrm{SU}(2)_\mathrm{L} \times \mathrm{U}(1)_\mathrm{Y}$ by the vacuum expectation value (VEV) of a SM-singlet scalar field in Σ: $\langle\Sigma\rangle = v_{24}\mathrm{diag}(2,2,2,-3,-3)$. The field Σ is decomposed around the VEV as

$$\Sigma^A{}_B = \begin{pmatrix} (\Sigma_8)^{\hat a}{}_{\hat b} + 2\left(v_{24} - \frac{1}{2\sqrt{15}}\Sigma_1\right)\delta^{\hat a}{}_{\hat b} & \frac{1}{\sqrt{2}}(\Sigma_G)^{\hat a}{}_\beta \\ \frac{1}{\sqrt{2}}(\Sigma_G^*)^\alpha{}_{\hat b} & (\Sigma_3)^\alpha_\beta - 3\left(v_{24} - \frac{1}{2\sqrt{15}}\Sigma_1\right)\delta^\alpha{}_\beta \end{pmatrix}, \tag{5}$$

where $\hat a, \hat b = 1, 2, 3$ and $\alpha, \beta = 1, 2$ are SU(3) and SU(2) indices, respectively. The spontaneous breaking of SU(5) typically provides the masses of the scalars Σ_1, Σ_3, and Σ_8 of the order of v_{24}, while $\Sigma_G^{(*)}$ corresponds to the massless would-be Nambu-Goldstone boson, which gives masses to the gauge bosons associated with the broken symmetries. These massive vector bosons are called X bosons.

B. Fermions

The SM fermions q_{Li}, u_{Ri}^c, d_{Ri}^c, ℓ_{Li}, and e_{Ri}^c are embedded into the **10** and $\bar{\mathbf{5}}$ representations as

$$(\Psi_{10i})^{AB} = \frac{1}{\sqrt{2}}\begin{pmatrix} \epsilon^{\hat a\hat b\hat c}(V_{QU})_i{}^k u_{Rk\hat c}^c & q_{Li}^{\hat a\beta} \\ -q_{Li}^{\hat b\alpha} & \epsilon^{\alpha\beta}(V_{QE})_i{}^k e_{Rk}^c \end{pmatrix},$$
$$(\Psi_{\bar 5i})_A = \begin{pmatrix} d_{Ri\hat a}^c & \epsilon_{\alpha\beta}(V_{DL})_i{}^k \ell_{Lk}^\beta \end{pmatrix}, \tag{6}$$

where i, k are the generation indices, and the totally antisymmetric tensors are defined as $\epsilon^{12} = \epsilon_{12} = 1$ and $\epsilon^{123} = \epsilon_{123} = 1$. Without loss of generality, one can rotate the basis of Ψ_{10} and $\Psi_{\bar 5}$ as

$$\Psi_{10} \to U_{10}\Psi_{10}, \qquad \Psi_{\bar 5} \to U_5\Psi_{\bar 5}, \tag{7}$$

where U_{10} and U_5 are arbitrary unitary matrices in the generation space. By using the degrees of freedom associated with the unitary rotations, we can take the basis where the up-type quarks and the charged leptons are in their mass eigenstates:

$$q_{Li} = \begin{pmatrix} \hat u_{Li} \\ (V_{\mathrm{CKM}})_i{}^j \hat d_{Lj} \end{pmatrix}, \qquad u_{Ri} = \hat u_{Ri}, \qquad d_{Ri} = \hat d_{Ri},$$
$$\ell_{Li} = \begin{pmatrix} \hat\nu_{Li} \\ \hat e_{Li} \end{pmatrix}, \qquad e_{Ri} = \hat e_{Ri}, \tag{8}$$

where the mass eigenstates are denoted with a hat, and V_{CKM} is the Cabibbo-Kobayashi-Maskawa (CKM) matrix in the Particle Data Group (PDG) phase convention [49,50]. Analogous to the CKM matrix that represents a mismatch of the bases in q_L, the unitary matrices V_{QU}, V_{QE}, and V_{DL} are introduced in Ψ_{10} and $\Psi_{\bar 5}$ as in Eq. (6).

C. Scalar spectrum and gauge coupling unification

The scalar Φ_5 is decomposed to the so-called color triplet Higgs $S_1^{(5)*}$ and the $\mathrm{SU}(2)_\mathrm{L}$ doublet $H^{(5)}$:

$$(\Phi_5)^A = \begin{pmatrix} S_1^{(5)*\hat a} \\ H^{(5)\alpha} \end{pmatrix}, \tag{9}$$

while the Φ_{45} consists of the scalars $\tilde S_1$, R_2^*, S_3^*, S_6^*, S_8, $H^{(45)}$, and $S_1^{(45)*}$ as

$$(\Phi_{45})^{\hat a\hat b}_{\hat c} = \frac{1}{\sqrt{2}}\epsilon^{\hat a\hat b\hat d}\left[(\eta_a)_{\hat c\hat d}S_6^{*a} - \frac{1}{2}\epsilon_{\hat c\hat d\hat e}S_1^{(45)*\hat e}\right],$$
$$(\Phi_{45})^{\hat a\hat b}_\gamma = \frac{1}{\sqrt{2}}\epsilon^{\hat a\hat b\hat d}R_{2\hat d\gamma}^*,$$
$$(\Phi_{45})^{\hat a\beta}_{\hat c} = \frac{1}{\sqrt{2}}\left[\frac{1}{\sqrt{2}}(\lambda_a)^{\hat a}{}_{\hat c}S_8^{a\beta} + \frac{1}{2\sqrt{3}}\delta^{\hat a}_{\hat c}H^{(45)\beta}\right],$$
$$(\Phi_{45})^{\alpha\beta}_{\hat c} = \frac{1}{\sqrt{2}}\epsilon^{\alpha\beta}\tilde S_{1\hat c},$$
$$(\Phi_{45})^{\alpha\hat b}_\gamma = \frac{1}{\sqrt{2}}\left(\frac{1}{\sqrt{2}}(\sigma_a)^\alpha{}_\gamma S_3^{*\hat b} - \frac{1}{2}\delta^\alpha_\gamma S_1^{(45)*\hat b}\right),$$
$$(\Phi_{45})^{\alpha\beta}_\gamma = -\frac{\sqrt{3}}{2\sqrt{2}}\epsilon^{\alpha\beta}\epsilon_{\gamma\delta}H^{(45)\delta}, \tag{10}$$

where σ_a $(a = 1,\ 2,\ 3)$ are the Pauli matrices, $\lambda_a(a = 1, 2, \ldots, 8)$ the Gell-Mann matrices, and $\eta_a(a = 1, 2, \ldots, 6)$ the symmetric matrices defined by

TABLE I. The decomposition of the scalar fields Σ, Φ_5, and Φ_{45} under the SM gauge groups.

Field	SU(5)	Field	$SU(3)_C$	$SU(2)_L$	$U(1)_Y$	Field	SU(5)	Field	$SU(3)_C$	$SU(2)_L$	$U(1)_Y$
Σ	**24**	Σ_1	**1**	**1**	0	Φ_{45}	**45**	$\tilde{S}_1$	$\bar{\mathbf{3}}$	**1**	4/3
		Σ_3	**1**	**3**	0			R_2^*	$\bar{\mathbf{3}}$	$\bar{\mathbf{2}}$	−7/6
		Σ_G	**3**	$\bar{\mathbf{2}}$	−5/6			S_3^*	**3**	**3**	−1/3
		Σ_G^*	$\bar{\mathbf{3}}$	**2**	5/6			S_6^*	$\bar{\mathbf{6}}$	**1**	−1/3
		Σ_8^*	**8**	**1**	0			S_8	**8**	**2**	1/2
Φ_5	**5**	$H^{(5)}$	**1**	**2**	1/2			$H^{(45)}$	**1**	**2**	1/2
		$S_1^{(5)*}$	**3**	**1**	−1/3			$S_1^{(45)*}$	**3**	**1**	−1/3

$$\{\eta_1,\eta_2,\eta_3,\eta_4,\eta_5,\eta_6\} = \left\{ \begin{pmatrix} 1 & 0 & 0 \\ 0 & 0 & 0 \\ 0 & 0 & 0 \end{pmatrix}, \begin{pmatrix} 0 & 0 & 0 \\ 0 & 1 & 0 \\ 0 & 0 & 0 \end{pmatrix}, \begin{pmatrix} 0 & 0 & 0 \\ 0 & 0 & 0 \\ 0 & 0 & 1 \end{pmatrix}, \frac{1}{\sqrt{2}}\begin{pmatrix} 0 & 1 & 0 \\ 1 & 0 & 0 \\ 0 & 0 & 0 \end{pmatrix}, \frac{1}{\sqrt{2}}\begin{pmatrix} 0 & 0 & 1 \\ 0 & 0 & 0 \\ 1 & 0 & 0 \end{pmatrix}, \frac{1}{\sqrt{2}}\begin{pmatrix} 0 & 0 & 0 \\ 0 & 0 & 1 \\ 0 & 1 & 0 \end{pmatrix} \right\}. \tag{11}$$

The decompositions of Σ, Φ_5, and Φ_{45} are summarized in Table I. Here the scalar $H^{(45)}$ ($S_1^{(45)}$) has the same quantum numbers under the SM gauge group as $H^{(5)}$ ($S_1^{(5)}$). Therefore, they can mix with each other, and we define the mass eigenstates H, H', H_C, and S_1 by introducing the mixing angles θ_H and θ_S and the phases δ_H and δ_S:

$$\begin{pmatrix} H \\ H' \end{pmatrix} = \begin{pmatrix} c_H & e^{-i\delta_H} s_H \\ -e^{i\delta_H} s_H & c_H \end{pmatrix} \begin{pmatrix} H^{(5)} \\ H^{(45)} \end{pmatrix},$$
$$\begin{pmatrix} H_C \\ S_1 \end{pmatrix} = \begin{pmatrix} c_S & e^{-i\delta_S} s_S \\ -e^{i\delta_S} s_S & c_S \end{pmatrix} \begin{pmatrix} S_1^{(5)} \\ S_1^{(45)} \end{pmatrix}, \tag{12}$$

where $c_H = \cos\theta_H$, $s_H = \sin\theta_H$, $c_S = \cos\theta_S$, and $s_S = \sin\theta_S$. The presence of the two doublet scalars allows us to explain the masses of the down-type quarks and the charged leptons simultaneously.

Owing to the symmetry breaking of SU(5) to the SM gauge groups, mass splitting may occur among the scalar fields embedded in the SU(5) multiplets. At least one $SU(2)_L$-doublet scalar has to be light to break the EW symmetry spontaneously below the TeV scale.[2] We assume that the scalar H is light and corresponds to the SM Higgs doublet.

It is well-known that the SM gauge couplings do not unify only by naive RG running in the SM. The mass splitting of the SU(5) scalar multiplets can improve the situation. We consider the scenario where some of the scalar fields, in addition to H, are much lighter than others. At the energy scale above the mass of an additional light scalar, the scalar contributes to the RG running of the gauge couplings. The gauge coupling unification is realized if an appropriate set of light scalars is considered. We define $\alpha_3(\mu)$, $\alpha_2(\mu)$, and $\alpha_1(\mu)$ as

$$\alpha_3(\mu) = \alpha_s(\mu) = \frac{g_s(\mu)^2}{4\pi}, \qquad \alpha_2(\mu) = \frac{g(\mu)^2}{4\pi},$$
$$\alpha_1(\mu) = \frac{5}{3}\frac{g'(\mu)^2}{4\pi}, \tag{13}$$

where g_s, g, and g' are the gauge couplings of $SU(3)_C$, $SU(2)_L$, and $U(1)_Y$, respectively, and μ is the renormalization scale. Our analysis assumes that the SM gauge couplings are unified at the scale M_X, i.e., $\alpha_3(M_X) = \alpha_2(M_X) = \alpha_1(M_X) \equiv \alpha_X(M_X)$, and all the scalar masses are not heavier than M_X. Then, above the M_X scale, all the scalars contribute to the running as complete SU(5) multiplets so that the coupling unification holds above M_X. We also make an ansatz that the mass of the X boson is equal to the unification scale M_X.

Solving the renormalization group equations (RGEs) in Appendix C with the unification assumption, we get the three relations,

$$\alpha_X^{-1}(M_X) = \alpha_3^{-1}(m_Z) - \left(\frac{B_{g_s}^{\rm SM}}{2\pi}\log\frac{M_X}{m_Z} + \sum_\phi \frac{B_{g_s}^\phi}{2\pi}\log\frac{M_X}{m_\phi} \right),$$
$$\alpha_X^{-1}(M_X) = \alpha_2^{-1}(m_Z) - \left(\frac{B_{g}^{\rm SM}}{2\pi}\log\frac{M_X}{m_Z} + \sum_\phi \frac{B_{g}^\phi}{2\pi}\log\frac{M_X}{m_\phi} \right),$$
$$\alpha_X^{-1}(M_X) = \alpha_1^{-1}(m_Z) - \frac{3}{5}\left(\frac{B_{g'}^{\rm SM}}{2\pi}\log\frac{M_X}{m_Z} + \sum_\phi \frac{B_{g'}^\phi}{2\pi}\log\frac{M_X}{m_\phi} \right), \tag{14}$$

[2]The EW symmetry breaking can also be driven by the VEV of Σ_3 below the TeV scale. However, we assume that Σ_3 does not develop a VEV since it causes a dangerous contribution to the ρ parameter.

TABLE II. Input values for the Z-boson mass m_Z, the gauge couplings $\alpha_s(m_Z)$ and $\alpha^{-1}(m_Z)$, the weak mixing angle $\sin^2\theta_W(m_Z)$, the quark masses, and the CKM parameters s_{ij} and δ, taken from Ref. [50]. Other parameters, such as the pole masses of the charged leptons m_e, m_μ, and m_τ, are also taken from Ref. [50].

Parameter	Value	Parameter	Value	Parameter	Value	Parameter	Value
m_Z	91.1876 GeV	$m_u(2\ \text{GeV})$	0.00216 GeV	$m_d(2\ \text{GeV})$	0.00467 GeV	s_{12}	0.22650
$\alpha_s(m_Z)$	0.1179	$m_c(m_c)$	1.27 GeV	$m_s(2\ \text{GeV})$	0.093 GeV	s_{13}	0.00361
$\alpha^{-1}(m_Z)$	127.952	m_t^{pole}	172.76 GeV	$m_b(m_b)$	4.18 GeV	s_{23}	0.04053
$\sin^2\theta_W(m_Z)$	0.23121					δ	1.196 rad

where m_Z is the Z-boson mass, ϕ is summed over all the relevant scalars, and the coefficients $B_{g_i}^{\text{SM}}$ and $B_{g_i}^{\phi}$ are given in Table IV. Eliminating $\alpha_X^{-1}(M_X)$ [51], one can get two independent equations,

$$\begin{aligned}&\frac{2}{5}\log\frac{m_{H_C}}{m_Z}+\frac{2}{5}\log\frac{m_{S_1}}{m_{H'}}+\frac{7}{5}\log\frac{m_{\tilde{S}_1}}{m_{S_3}}+\frac{4}{5}\log\frac{m_{R_2}}{m_{S_3}}\\&\quad+\frac{9}{5}\log\frac{m_{S_6}}{m_{S_3}}+\frac{4}{5}\log\frac{m_{S_8}}{m_{S_3}}+\log\frac{m_{\Sigma_8}}{m_{\Sigma_3}}\\&\quad=2\pi[-2\alpha_3^{-1}(m_Z)+3\alpha_2^{-1}(m_Z)-\alpha_1^{-1}(m_Z)]\\&\quad\simeq 79.8,\end{aligned}\tag{15}$$

$$\begin{aligned}&44\log\frac{M_X}{m_Z}+6\log\frac{m_{S_3}}{m_{R_2}}+\log\frac{m_{S_6}}{m_{\tilde{S}_1}}+4\log\frac{m_{S_8}}{m_{\tilde{S}_1}}+\log\frac{m_{\Sigma_3}m_{\Sigma_8}}{M_X^2}\\&\quad=2\pi[-2\alpha_3^{-1}(m_Z)-3\alpha_2^{-1}(m_Z)+5\alpha_1^{-1}(m_Z)]\\&\quad\simeq 1193,\end{aligned}\tag{16}$$

where the gauge couplings at $\mu=m_Z$ are evaluated for six active quark flavors [52] with the input values shown in Table II.

As a general property, the S_3 contribution improves the gauge coupling unification [18]. In the case that only the Higgs boson and S_3 are lighter than M_X in the scalar sector, the gauge coupling unification occurs at $M_X\sim\mathcal{O}(10^{14}\ \text{GeV})$ with $m_{S_3}\sim\mathcal{O}(10^8\ \text{GeV})$. However, M_X is severely constrained by proton decay search experiments, since contributions from the GUT gauge-boson exchange generate the dimension-six operators relevant to the proton decay. Then the proton lifetime is naively expected as [7,53]

$$\tau_p\sim\frac{M_X^4}{\alpha_X^2 m_p^5},\tag{17}$$

where m_p is the mass of proton, and one finds a naive lower bound as

$$M_X>5\times10^{15}\ \text{GeV},\tag{18}$$

by using the experimental lower limit on the lifetime $\tau(p\to\pi^0e^+)>2.4\times10^{34}$ years [54] and $\alpha_X^2\sim\mathcal{O}(10^{-3})$.

In order to avoid the rapid proton decay by making M_X much heavier, we assume that S_6, S_8, and Σ_8, in addition to S_3, are lighter than the unification scale M_X. With their contributions to the RGEs of the gauge couplings, M_X can be significantly heavier with keeping the coupling unification. Therefore, we consider a scenario where the masses of S_6, S_8, and Σ_8 are below M_X. For simplicity, we assume that the other scalar components, except for the SM-like Higgs doublet H, are as heavy as M_X.

Let us explain in more detail the masses of the other scalars embedded in the GUT representations. The mass parameter m_H^2 associated with the SM-like Higgs doublet H is of the order of the weak scale according to the LHC measurements, while the other scalars associated with the **5** and **45** representations obey the mass relation given in Eq. (A13). We simply choose that Σ_1, Σ_3, H', H_C, S_1, and $\tilde{S}_1$ have a common mass M_X. As a consequence, the mass of R_2 is determined as $m_{R_2}^2\approx(2+4s_H^2)M_X^2/3$, where s_H is the sine of the mixing angle defined in Eq. (12). For $s_H^2<1/4$, m_{R_2} is lighter than M_X.

In Fig. 1(a), the contours of M_X and m_{Σ_8} are shown in the parameter space of m_{S_3} and $m_{S_6}=m_{S_8}$. The gauge coupling unification favors rather light S_3, which can be as light as a TeV scale. The light gray regions are for $M_X<3\times10^{15}$ GeV, which is disfavored by the proton decay search as mentioned above. For example, if we take $m_{S_3}=2$ TeV, $m_{S_6}=m_{S_8}=m_{\Sigma_8}=5.2\times10^6$ GeV, and $\cot\theta_H=50$, the gauge coupling unification is realized at $M_X=9.7\times10^{16}$ GeV as shown in Fig. 1(b).

In the phenomenological analysis, we use a benchmark scenario with the following mass spectrum:

(1) The masses of the quarks and leptons, the SM gauge bosons, and the SM-like Higgs boson H are set to be consistent with their measurements;
(2) S_3 has a TeV-scale mass: $m_{S_3}\sim\mathcal{O}(10^3\ \text{GeV})$;
(3) S_6, S_8, and Σ_8 have intermediate masses, and we set them to an identical scale, i.e., $m_{S_6}=m_{S_8}=m_{\Sigma_8}\equiv M_I\sim\mathcal{O}(10^6\ \text{GeV})$;
(4) The other particles including the X bosons have masses of the order of the GUT scale M_X.

D. Yukawa couplings

Below the GUT scale, the Yukawa interactions with the scalars H, S_3, S_6, and S_8 are given by

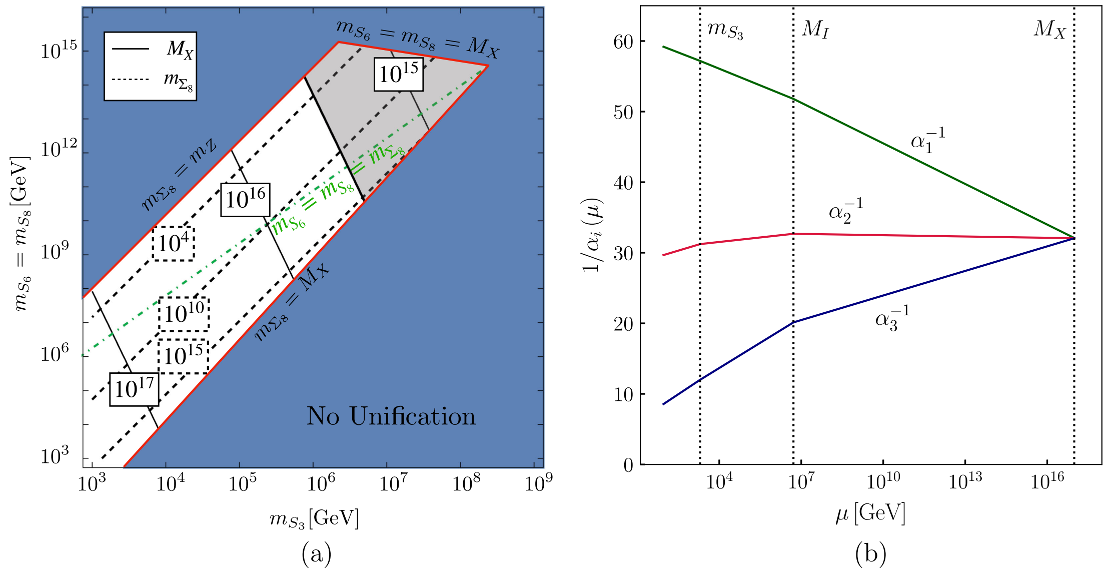

FIG. 1. (a) The contours of M_X (solid) and m_{Σ_8} (dashed) in the unit of GeV for realizing the coupling unification in the plane of m_{S_3} and $m_{S_6} = m_{S_8}$ for $\cot\theta_H = 50$. In the blue shaded region, the gauge coupling unification does not occur by RG running. The light gray region is disfavored by the proton decay experiments because M_X is too small. The green dot-dashed line corresponds to the case with $m_{S_6} = m_{S_8} = m_{\Sigma_8}$. (b) RG runnings of the gauge couplings for $m_{S_3} = 2$ TeV, $m_{S_6} = m_{S_8} = m_{\Sigma_8} \equiv M_I = 5.2 \times 10^6$ GeV, and $\cot\theta_H = 50$.

$$
\begin{aligned}
-\mathcal{L}_Y = {}& (Y_U)_{ij}\epsilon_{\alpha\beta}\bar{u}_{R\hat{a}i}H^\alpha q^{\hat{a}\beta}_{Lj} + (Y_D)_{ij}\bar{d}_{R\hat{a}i}H^*_\alpha q^{\hat{a}\alpha}_{Lj} + (Y_E)_{ij}\bar{e}_{Ri}H^*_\alpha \ell^\alpha_{Lj} + \frac{(Y_3^{QQ})_{ij}}{2}\epsilon_{\hat{a}\hat{b}\hat{c}}\epsilon_{\alpha\beta}\bar{q}^{c\hat{a}\alpha}_{Li}(\sigma^a)^\beta{}_\gamma S_3^{*a\hat{b}} q^{\hat{c}\gamma}_{Lj} \\
& + (Y_3^{QL})_{ij}\epsilon_{\alpha\beta}\bar{q}^{c\hat{a}\gamma}_{Li}(\sigma_a)^\alpha{}_\gamma S^a_{3\hat{a}}\ell^\beta_{Lj} + \frac{(Y_6^{QQ})_{ij}}{2}\epsilon_{\alpha\beta}\bar{q}^{c\hat{a}\alpha}_{Li}(\eta^A)_{\hat{a}\hat{b}}S_6^{A*}q^{\hat{b}\beta}_{Lj} + (Y_6^{DU})_{ij}\bar{d}_{R\hat{a}i}(\eta^A)^{\hat{a}\hat{b}}S_6^A u^c_{R\hat{b}j} \\
& + (Y_8^{UQ})_{ij}\epsilon_{\alpha\beta}\bar{u}_{R\hat{a}i}(\lambda^A)^{\hat{a}}{}_{\hat{b}}S_8^{A\alpha}q^{\hat{b}\beta}_{Lj} + (Y_8^{DQ})_{ij}\bar{d}_{R\hat{a}i}(\lambda^A)^{\hat{a}}{}_{\hat{b}}S^{A*}_{8\alpha}q^{\hat{b}\alpha}_{Lj} + \text{H.c.},
\end{aligned}
\tag{19}
$$

where the first three terms lead to the fermion mass terms after the Higgs field H acquires a VEV at the EW scale. The **45** scalar plays an essential role in reproducing the masses of the SM fermions. If the **45** scalar is absent, the Yukawa matrices must obey a condition $Y_E = V_{QE}^T Y_D^T V_{DL}$ at the GUT scale. This condition conflicts with the low-energy values of the masses of the down-type quarks and the charged leptons. In the current model, this problem is solved by the presence of the Yukawa coupling Y_{45}^D. Because the SM-like Higgs field H is a mixture of $H^{(5)}$ and $H^{(45)}$ as in Eq. (12), the Yukawa matrices Y_U, Y_D, and Y_E are given at the GUT scale by

$$
\begin{aligned}
Y_U &= -\frac{1}{2}V_{QU}^T\left(c_H Y_5^U + \sqrt{\frac{2}{3}}e^{i\delta_H}s_H Y_{45}^U\right)^T, \\
Y_D &= -\frac{1}{\sqrt{2}}\left(c_H Y_5^D - \frac{1}{2\sqrt{6}}e^{-i\delta_H}s_H Y_{45}^D\right)^T, \\
Y_E &= -\frac{1}{\sqrt{2}}V_{QE}^T\left(c_H Y_5^D + \frac{\sqrt{3}}{2\sqrt{2}}e^{-i\delta_H}s_H Y_{45}^D\right)V_{DL},
\end{aligned}
\tag{20}
$$

which can lead to realistic Yukawa matrices at the low energy. Moreover, the GUT-scale matching conditions for the other couplings in Eq. (19) read as

$$
\begin{aligned}
Y_3^{QQ} &= \frac{1}{2}Y_{45}^U, \qquad Y_6^{QQ} = -\frac{1}{\sqrt{2}}Y_{45}^U, \qquad Y_8^{UQ} = -\frac{1}{2}V_{QU}^T Y_{45}^U, \\
Y_3^{QL} &= -\frac{1}{2\sqrt{2}}Y_{45}^D V_{DL}, \qquad Y_6^{DU} = \frac{1}{2}(Y_{45}^D)^T V_{QU}, \\
Y_8^{DQ} &= \frac{1}{2\sqrt{2}}(Y_{45}^D)^T.
\end{aligned}
\tag{21}
$$

The scalar S_3 couples to a quark and a lepton simultaneously and thus is a leptoquark. The RGEs for these couplings are given in Appendix C.

Let us count the physical degrees of freedom in the Yukawa sector. In the general case, there are four Yukawa matrices Y_5^U, Y_{45}^U, Y_5^D, and Y_{45}^D in the GUT Lagrangian. Since Y_5^U and Y_{45}^U are symmetric and antisymmetric matrices, respectively, the four matrices contain 54 parameters in total. By the redefinitions of the fermion fields by U_{10} and U_5 in Eq. (7), 18 degrees of freedom out of the

54 can be eliminated. Thus there remain 36 physical parameters in the Yukawa matrices. Taking the basis where the up-type quarks and the charged leptons are their mass eigenstates, the Yukawa matrices Y_5^U, Y_{45}^U, Y_5^D, and Y_{45}^D are written as

$$\begin{aligned} Y_5^U &= -\frac{1}{c_H}(V_{QU}^*\hat{Y}_U + \hat{Y}_U V_{QU}^\dagger),\\ Y_{45}^U &= \frac{\sqrt{3}}{\sqrt{2}e^{i\delta_H}s_H}(V_{QU}^*\hat{Y}_U - \hat{Y}_U V_{QU}^\dagger),\\ Y_5^D &= -\frac{1}{2\sqrt{2}c_H}(3V_{\rm CKM}^*\hat{Y}_D + V_{QE}^*\hat{Y}_E V_{DL}^\dagger),\\ Y_{45}^D &= \frac{\sqrt{3}}{e^{-i\delta_H}s_H}(V_{\rm CKM}^*\hat{Y}_D - V_{QE}^*\hat{Y}_E V_{DL}^\dagger), \end{aligned} \tag{22}$$

where $\hat{Y}_U$, $\hat{Y}_D$, and $\hat{Y}_E$ represent diagonal matrices in the mass basis. It is noted that an overall phase in V_{QU} and three phases in V_{QE} (and/or V_{DL}) can be removed by $\mathrm{U}(1)_B$, $\mathrm{U}(1)_e$, $\mathrm{U}(1)_\mu$, and $\mathrm{U}(1)_\tau$ transformations. The right-hand sides of Eq. (22) then contain nine eigenvalues in $\hat{Y}_U$, $\hat{Y}_D$, and $\hat{Y}_E$, three mixing angles and one phase in $V_{\rm CKM}$, eight parameters in V_{QU}, and fifteen ones in V_{QE} and V_{DL}.

In general, the scalar S_3 can have two types of Yukawa couplings, Y_3^{QQ} and Y_3^{QL}, and the combination of these couplings leads to baryon-number-violating dimension-six operators, which cause too fast proton decay. For example, the bound from $p\to\pi^0 e^+$ is estimated as

$$|(Y_3^{QQ})_{12}(Y_3^{QL})_{11}(V_{\rm CKM})_2{}^1| \lesssim 10^{-25}\left(\frac{m_{S_3}}{2\ \mathrm{TeV}}\right)^2. \tag{23}$$

Because $(Y_3^{QL})_{11}\sim y_d/s_H$ with y_d being the Yukawa coupling for down quark, this condition implies a strong upper bound on $(Y_{45}^U)_{12}$:

$$|(Y_{45}^U)_{12}| \lesssim 10^{-20}\left(\frac{m_{S_3}}{2\ \mathrm{TeV}}\right)^2 s_H. \tag{24}$$

Other components in Y_{45}^U also have to be highly suppressed to avoid the constraints from the proton decay. As explained in Appendix C, the coupling Y_3^{QQ} in Eq. (19) is forbidden in the whole range of the renormalization scale by an accidental global symmetry $U(1)_B\times U(1)_L$ if Y_3^{QQ} is once set to be zero at the GUT scale. Therefore, in the following, we make an ansatz that $Y_{45}^U=0$ at the GUT scale.

We here show a parametrization for the mixing matrices V_{QU}, V_{QE}, and V_{DL}. According to the matching condition in Eq. (22), the ansatz $Y_{45}^U=0$ at the GUT scale requires that V_{QU} should be a diagonal phase matrix:

$$V_{QU} = \begin{pmatrix} 1 & 0 & 0\\ 0 & e^{i\alpha_2^{QU}} & 0\\ 0 & 0 & e^{i\alpha_3^{QU}} \end{pmatrix}. \tag{25}$$

The other two matrices V_{DL} and V_{QE} can be parametrized as

$$\begin{aligned} V_{QE} &= V_{\rm CKM}\begin{pmatrix} 1 & 0 & 0\\ 0 & e^{i\alpha_2^{QE}} & 0\\ 0 & 0 & e^{i\alpha_3^{QE}} \end{pmatrix}\hat{V}_{QE},\\ V_{DL} &= \begin{pmatrix} 1 & 0 & 0\\ 0 & e^{i\alpha_2^{DL}} & 0\\ 0 & 0 & e^{i\alpha_3^{DL}} \end{pmatrix}\hat{V}_{DL}\begin{pmatrix} e^{i\beta_1^{DL}} & 0 & 0\\ 0 & e^{i\beta_2^{DL}} & 0\\ 0 & 0 & e^{i\beta_3^{DL}} \end{pmatrix}, \end{aligned} \tag{26}$$

where $\hat{V}_{QE}$ and $\hat{V}_{DL}$ are the 3×3 unitary matrices parametrized by three angles and one phase as the CKM matrix, and $V_{\rm CKM}$ is extracted in V_{QE}.

We define the coupling $\bar{Y}_3^{QL}$ in the mass basis of the down-type quarks and the charged leptons:

$$\bar{Y}_3^{QL} = V_{\rm CKM}^T Y_3^{QL} = -\frac{\sqrt{6}}{4e^{-i\delta_H}s_H}(\hat{Y}_D V_{DL} - \bar{V}_{QE}^*\hat{Y}_E), \tag{27}$$

where $\bar{V}_{QE}=V_{\rm CKM}^\dagger V_{QE}$. The mixings in $\bar{V}_{QE}$ (V_{DL}) cause flavor transitions between different generations of the down-type quarks (the charged leptons). To suppress dangerous contributions to flavor-changing processes associated with the first generation [44,47], such as $K\to\pi\nu\bar{\nu}$ and $\mu^-\to e^-\gamma$, we assume that $\hat{V}_{QE}$ and $\hat{V}_{DL}$ have only the mixing between the second and the third generations at the GUT scale:

$$\begin{aligned} \hat{V}_{QE} &= \begin{pmatrix} 1 & 0 & 0\\ 0 & \cos\theta_{QE} & \sin\theta_{QE}\\ 0 & -\sin\theta_{QE} & \cos\theta_{QE} \end{pmatrix},\\ \hat{V}_{DL} &= \begin{pmatrix} 1 & 0 & 0\\ 0 & \cos\theta_{DL} & \sin\theta_{DL}\\ 0 & -\sin\theta_{DL} & \cos\theta_{DL} \end{pmatrix}, \end{aligned} \tag{28}$$

where the mixing angles θ_{QE} and θ_{DL} are varied from 0 to $\pi/2$. The three Yukawa matrices Y_{10}, Y_5, and Y_{45}^D are then determined at the GUT scale by the thirteen input parameters in addition to $\hat{Y}_U$, $\hat{Y}_D$, $\hat{Y}_E$, and $V_{\rm CKM}$, i.e., the two mixing angles θ_{QE} and θ_{DL}, the nine phases in V_{QU}, V_{QE}, and V_{DL}, and the two parameters $s_H=\sin\theta_H$ and δ_H in the Higgs sector.

The Y_3^{QL} term in Eq. (19) is decomposed in terms of the fields in the EW broken phase as follows [36]:

$$\mathcal{L}_Y = -\bar{\hat{u}}_L^c Y_3^{QL} \hat{e}_L S_3^{1/3} - \sqrt{2}\bar{\hat{d}}_L^c \bar{Y}_3^{QL} \hat{e}_L S_3^{4/3} + \sqrt{2}\bar{\hat{u}}_L^c Y_3^{QL} \hat{\nu}_L S_3^{-2/3} - \bar{\hat{d}}_L^c \bar{Y}_3^{QL} \hat{\nu}_L S_3^{1/3} + \text{H.c.}, \tag{29}$$

where the hatted quark and lepton fields represent the mass eigenstates as in Eq. (8), and S_3^Q denotes a charge eigenstate with charge Q defined in the matrix form

$$\frac{1}{\sqrt{2}}(\sigma^A)^\alpha{}_\beta (S_3)^A_{\hat{c}} = \begin{pmatrix} \frac{1}{\sqrt{2}}(S_3^{1/3})_{\hat{c}} & (S_3^{4/3})_{\hat{c}} \\ (S_3^{-2/3})_{\hat{c}} & -\frac{1}{\sqrt{2}}(S_3^{1/3})_{\hat{c}} \end{pmatrix}. \tag{30}$$

III. PHENOMENOLOGICAL ANALYSIS

A. Input parameters

We study low-energy phenomenology of the SU(5) GUT model proposed in the last section, where there is an S_3 leptoquark with a TeV-scale mass. As explained in Sec. II D the S_3 leptoquark has the Yukawa couplings with the left-handed quarks and the left-handed leptons, which lead to rich flavor phenomenology at the low-energy scale. In particular, the S_3 couplings generate processes with lepton-flavor violation (LFV) and lepton-flavor-universality violation (LFUV), while such exotic flavor processes are severely constrained by experiments. Our aim is to investigate whether current and future flavor experiments have a potential to explore our GUT-inspired scenario. The S_3 Yukawa matrix Y_3^{QL} in our scenario cannot have an arbitrary structure unlike that in phenomenological leptoquark models where S_3 is introduced by hand. The coupling Y_3^{QL} originates from Y_{45}^D in the GUT Lagrangian, and Y_{45}^D also contribute to the SM Yukawa couplings Y_D and Y_E as in Eq. (20), which could help to explain the observed masses of the down-type quarks and the charged leptons. Thus, nontrivial correlations are expected among flavor observables where the S_3 leptoquark contributes.

The parameters in the GUT model, such as the Yukawa couplings Y_5^U, Y_5^D, and Y_{45}^D and the mixing matrices V_{QE} and V_{DL}, are constrained by the low-energy values of the SM fermion masses and the CKM matrix elements. We use the fermion masses and the CKM matrix elements listed in Table II as inputs, and calculate the running masses at the EW scale by taking into account QCD corrections for quarks with RunDec [55,56] and one-loop QED corrections for charged leptons [52]. The masses and the CKM matrix elements as well as the gauge couplings at the EW scale are then evolved up to the GUT scale with the one-loop RGEs in Appendix C, where the Yukawa couplings Y_3^{QL}, Y_6^{DU}, and Y_8^{DQ} are neglected at this stage. At the GUT scale we calculate the couplings Y_5^U, Y_5^D, Y_{45}^D with Eq. (22) by inputting V_{QE} and V_{DL}, δ_H, and s_H. The couplings Y_U, Y_D, Y_E, Y_3^{QL}, Y_6^{DU}, and Y_8^{DQ} are calculated at the GUT scale with Eqs. (20) and (21), and we then perform the RG evolution from the GUT scale to the low scale. The fermion masses and the CKM elements at the low scale obtained from this procedure are different from the original values due to the effects from Y_3^{QL}, Y_6^{DU}, and Y_8^{DQ}. We iterate the RG running with the obtained values of Y_3^{QL}, Y_6^{DU}, and Y_8^{DQ} together with the original values of the SM fermion masses and the CKM elements until the difference in the masses and the CKM elements becomes small enough. In this way we can determine a set of the GUT parameters that are consistent with the low-energy values of the SM fermion masses, the CKM matrix elements, and the gauge couplings.

We fix the mass of the S_3 leptoquark to be $m_{S_3} = 2$ TeV to avoid constraints from high-p_T searches at the LHC [57]. In addition, there are the thirteen arbitrary parameters: the three mixing angles θ_{QE}, θ_{DL}, and θ_H, and the ten phases α_2^{QU}, α_3^{QU}, α_2^{QE}, α_3^{QE}, α_2^{DL}, α_3^{DL}, β_1^{DL}, β_2^{DL}, β_3^{DL}, and δ_H. In general the Yukawa couplings $(\bar{Y}_3^{QL})_{ij}$ in Eq. (27) become larger for a smaller Higgs mixing angle θ_H. We choose $\cot\theta_H = 50$ as a benchmark scenario, while the other parameters are varied arbitrarily in their physical domain. The S_3 contributions to the flavor observables considered below are reduced by taking a heavier m_{S_3} and/or a smaller $\cot\theta_H$.

B. Leptoquark couplings

The Yukawa couplings $(\bar{Y}_3^{QL})_{ij}$ of the S_3 leptoquark are constrained by the GUT relation in Eq. (27) to accommodate with the measured masses of the down-type quarks and the charged leptons at the low-energy scale. The RG effects from the GUT scale M_X to the S_3 mass scale m_{S_3} are shown in Fig. 2. It is noted that the magnitudes of the couplings typically enhance at the lower scale. In particular, the 22 coupling is increased by about a factor of 2, receiving one-loop corrections with the other couplings. Therefore, the inclusion of the RG evolution is essential to study low-energy phenomenology associated with the 22 coupling, such as $b \to s\mu^+\mu^-$ processes.

According to Fig. 2, the couplings with the second-generation fermions are typically smaller than those with the third-generation ones:

$$|(\bar{Y}_3^{QL})_{22}| \ll |(\bar{Y}_3^{QL})_{23}| \sim |(\bar{Y}_3^{QL})_{32}| \lesssim |(\bar{Y}_3^{QL})_{33}|. \tag{31}$$

On the other hand, the couplings with the first-generation fermions are negligibly small due to our ignorance of the corresponding mixings in Eq. (28).

C. Matching onto low-energy theory

The gauge couplings and the Yukawa couplings in Eq. (19) at the GUT scale are evolved down to the mass

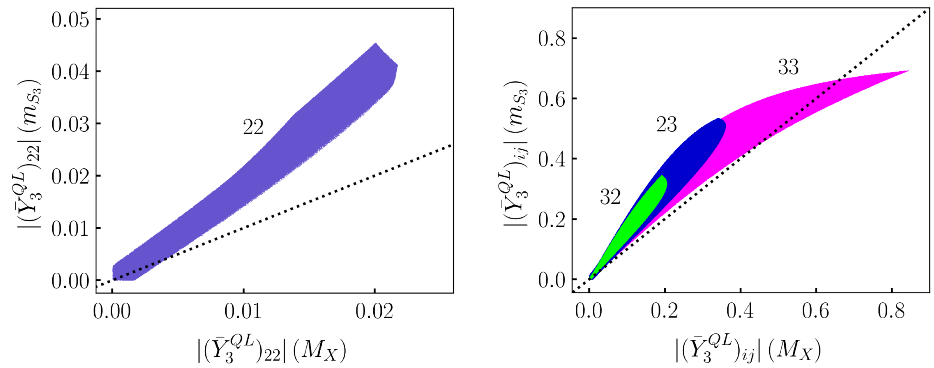

FIG. 2. Comparisons of the Yukawa couplings of the S_3 leptoquark at the GUT scale $\mu = M_X$ and at the S_3 mass scale $\mu = m_{S_3}$, where they are identical to each other on the dotted lines.

scale m_{S_3} using the RGEs given in Appendix C, where S_6, S_8, and Σ_8 are decoupled at the intermediate scale M_I. The leptoquark S_3 is then decoupled at the scale m_{S_3}, and the theory is matched onto the Standard Model Effective Field Theory (SMEFT). The corresponding tree-level matching conditions are presented in Refs. [58,59], while the one-loop ones are calculated in Ref. [60]. In addition, the one-loop anomalous dimensions in the SMEFT are found in Refs. [61–63].

We adopt the dimension-six SMEFT operators in the so-called Warsaw basis [64], where the Lagrangian in the SMEFT is given by the sum of the renormalizable SM Lagrangian and terms with higher-dimensional operators $\mathcal{O}_i$: $\mathcal{L}_{\rm SMEFT} = \mathcal{L}_{\rm SM} + \sum_i \mathcal{C}_i \mathcal{O}_i$. At the tree level, only the semileptonic operators $[\mathcal{O}_{\ell q}^{(1)}]_{ijkl} = (\overline{\ell}_{Li}\gamma^\mu \ell_{Lj})(\bar{q}_{Lk}\gamma_\mu q_{Ll})$ and $[\mathcal{O}_{\ell q}^{(3)}]_{ijkl} = (\overline{\ell}_{Li}\gamma^\mu \sigma_a \ell_{Lj})(\bar{q}_{Lk}\gamma_\mu \sigma_a q_{Ll})$ are generated by integrating out the S_3 leptoquark, where the corresponding Feynman diagram above the S_3 mass scale is presented in Fig. 3(a), and that below the S_3 mass scale, i.e., in the SMEFT, is in Fig. 3(b). The tree-level matching conditions for the semileptonic operators are given by

$$\left[\mathcal{C}_{\ell q}^{(1)}(m_{S_3})\right]_{ijkl} = 3\left[\mathcal{C}_{\ell q}^{(3)}(m_{S_3})\right]_{ijkl} = \frac{3}{4m_{S_3}^2}(Y_3^{QL*})_{ki}(Y_3^{QL})_{lj}, \tag{32}$$

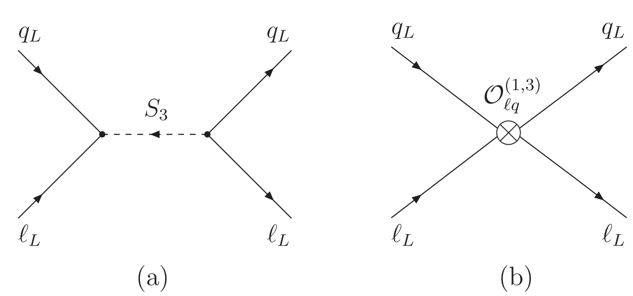

FIG. 3. Diagrams for the tree-level matching at the S_3 mass scale. Corresponding diagrams (a) in the model above the S_3 mass scale, and (b) in the SMEFT below the S_3 mass scale.

where Y_3^{QL} in the right-hand side is the S_3 Yukawa coupling at the S_3 mass scale, obtained from the coupling at the GUT scale in Eq. (21) applying the RG evolution. We also define the coefficients $\bar{\mathcal{C}}_{\ell q}^{(1,3)}$ in the mass basis of the down-type quarks and the charged leptons, and their matching conditions read as

$$\left[\bar{\mathcal{C}}_{\ell q}^{(1)}(m_{S_3})\right]_{ijkl} = 3\left[\bar{\mathcal{C}}_{\ell q}^{(3)}(m_{S_3})\right]_{ijkl} = \frac{3}{4m_{S_3}^2}(\bar{Y}_3^{QL*})_{ki}(\bar{Y}_3^{QL})_{lj}, \tag{33}$$

where $\bar{Y}_3^{QL} = V_{\rm CKM}^T Y_3^{QL}$.

The SMEFT coefficients in Eqs. (32) and (33) are evolved down to the EW scale, at which the SMEFT is matched onto the low-energy effective field theory (LEFT) [65] by integrating out the EW gauge bosons, the Higgs boson, and the top quark. The LEFT operators used in our phenomenological analysis are listed in Eq. (D2). The tree-level matching conditions for the coefficients L_i in the LEFT Lagrangian of Eq. (D1) can be found in Refs. [65,66], while the one-loop ones are calculated in Ref. [67]. Moreover, the RGEs for L_i are calculated at the one-loop level in Refs. [68,69]. We decompose L_i into the sum of SM and new physics (NP) contributions as $L_i = L_i^{\rm SM} + L_i^{\rm NP}$. In the current model only the semileptonic operators with the left-handed fermions are generated through the tree-level matching. For example, we have the following coefficients at the weak scale $\mu = m_Z$:

$$\left[L_{\nu d}^{V,LL}(m_Z)\right]_{ijkl}^{\rm NP} = \left[\bar{\mathcal{C}}_{\ell q}^{(1)}(m_Z)\right]_{ijkl} - \left[\bar{\mathcal{C}}_{\ell q}^{(3)}(m_Z)\right]_{ijkl}, \tag{34}$$

$$\left[L_{ed}^{V,LL}(m_Z)\right]_{ijkl}^{\rm NP} = \left[\bar{\mathcal{C}}_{\ell q}^{(1)}(m_Z)\right]_{ijkl} + \left[\bar{\mathcal{C}}_{\ell q}^{(3)}(m_Z)\right]_{ijkl}, \tag{35}$$

$$\left[L_{\nu edu}^{V,LL}(m_Z)\right]_{ijkl}^{\rm NP} = 2V_{wk}^*\left[\mathcal{C}_{\ell q}^{(3)}(m_Z)\right]_{ijwl}, \tag{36}$$

where V_{wk} denotes a CKM matrix element.

In our numerical analysis, we also include one-loop corrections to the matching onto the SMEFT, the RG evolution from $\mu = m_{S_3}$ to $\mu = m_Z$, the matching onto the LEFT, and the RG evolution from $\mu = m_Z$ to the lower energy scale. Let us consider the LEFT coefficient $L_{ed}^{V,LL}$ for $b \to s$ processes as an example. Solving the RGEs in the leading-logarithmic approximation, the coefficient $L_{ed}^{V,LL}$ is given at the bottom scale $\mu = m_b$ by

$$\begin{aligned}\left[L_{ed}^{V,LL}(m_b)\right]_{ij23}^{\mathrm{NP}} &= \frac{(\bar{Y}_3^{QL})^*_{2i}(\bar{Y}_3^{QL})_{3j}}{m_{S_3}^2}\left\{1-\frac{\alpha}{2\pi}\log\left(\frac{m_{S_3}^2}{m_b^2}\right)+\frac{g^2(1-4c_W^4)}{32\pi^2 c_W^2}\left[\log\left(\frac{m_{S_3}^2}{m_Z^2}\right)+\frac{11}{6}\right]\right\} \\ &+\frac{y_t^2}{64\pi^2}\left\{2V_{ts}^*V_{tb}\frac{(Y_3^{QL})^*_{3i}(Y_3^{QL})_{3j}}{m_{S_3}^2}+\left[V_{ts}^*\frac{(Y_3^{QL})^*_{3i}(\bar{Y}_3^{QL})_{3j}}{m_{S_3}^2}+V_{tb}\frac{(\bar{Y}_3^{QL})^*_{2i}(Y_3^{QL})_{3j}}{m_{S_3}^2}\right]I_{ed}(x_t)\right\} \\ &-\frac{3(N_c+1)}{8}\left[\frac{(\bar{Y}_3^{QL\dagger}\bar{Y}_3^{QL}\bar{Y}_3^{QL\dagger})_{i2}(\bar{Y}_3^{QL})_{3j}}{(4\pi)^2 m_{S_3}^2}+\frac{(\bar{Y}_3^{QL})^*_{2i}(\bar{Y}_3^{QL}\bar{Y}_3^{QL\dagger}\bar{Y}_3^{QL})_{3j}}{(4\pi)^2 m_{S_3}^2}\right] \\ &-\frac{5}{4}\frac{(\bar{Y}_3^{QL\dagger}\bar{Y}_3^{QL})_{ij}(\bar{Y}_3^{QL}\bar{Y}_3^{QL\dagger})_{32}}{(4\pi)^2 m_{S_3}^2}-\delta_{ij}\frac{\alpha}{6\pi}\frac{(\bar{Y}_3^{QL}\bar{Y}_3^{QL\dagger})_{32}}{m_{S_3}^2}\left[\log\left(\frac{m_{S_3}^2}{m_b^2}\right)-\frac{19}{12}\right], \end{aligned} \tag{37}$$

where $c_W = \cos\theta_W$ is the cosine of the Weinberg angle, y_t represents the SM Yukawa coupling of the top quark, $x_t = m_t^2/m_W^2$ with m_t and m_W being the masses of the top quark and the W boson, $N_c = 3$ is the number of colors, α is the electromagnetic coupling, and $I_{ed}(x)$ is the loop function defined by

$$I_{ed}(x) = -\log\left(\frac{m_{S_3}^2}{m_W^2}\right) - \frac{3(x+1)}{2(x-1)} + \frac{x^2-2x+4}{(x-1)^2}\log x. \tag{38}$$

In Eq. (37), the S_3 couplings Y_3^{QL} and $\bar{Y}_3^{QL}$ should be understood as those evaluated at the S_3 mass scale. The one-loop expressions for the other LEFT coefficients relevant to our analysis are given in Appendix D.

It is convenient to convert the LEFT coefficients of the $b \to s$ semileptonic operators into the coefficients in the weak Hamiltonian [70]:

$$\begin{aligned}\mathcal{H}_W = -\frac{4G_F}{\sqrt{2}}\frac{\alpha}{4\pi}V_{ts}^*V_{tb}\Big[&[C_{9V}]_{ij}(\bar{\hat{s}}_L\gamma^\mu\hat{b}_L)(\bar{\hat{e}}_i\gamma_\mu\hat{e}_j) \\ &+[C_{10A}]_{ij}(\bar{\hat{s}}_L\gamma^\mu\hat{b}_L)(\bar{\hat{e}}_i\gamma_\mu\gamma_5\hat{e}_j) \\ &+[C_L]_{ij}(\bar{\hat{s}}_L\gamma^\mu\hat{b}_L)(\bar{\hat{\nu}}_i\gamma_\mu(1-\gamma_5)\hat{\nu}_j)\Big]+\mathrm{H.c.},\end{aligned} \tag{39}$$

where G_F is the Fermi constant, and the NP contributions to the coefficients at the scale μ are related to the LEFT ones as

$$\left[C_{9V}^{\mathrm{NP}}(\mu)\right]_{ij} = \frac{\pi}{\sqrt{2}G_F\alpha V_{ts}^*V_{tb}}\left(\left[L_{ed}^{V,LL}(\mu)\right]_{ij23}^{\mathrm{NP}} + \left[L_{de}^{V,LR}(\mu)\right]_{23ij}^{\mathrm{NP}}\right), \tag{40}$$

$$[C_{10A}^{\mathrm{NP}}(\mu)]_{ij} = \frac{\pi}{\sqrt{2}G_F\alpha V_{ts}^*V_{tb}}\left(-\left[L_{ed}^{V,LL}(\mu)\right]_{ij23}^{\mathrm{NP}} + \left[L_{de}^{V,LR}(\mu)\right]_{23ij}^{\mathrm{NP}}\right), \tag{41}$$

$$[C_L^{\mathrm{NP}}]_{ij} = \frac{\pi}{\sqrt{2}G_F\alpha V_{ts}^*V_{tb}}\left[L_{\nu d}^{V,LL}\right]_{ij23}^{\mathrm{NP}}. \tag{42}$$

The argument μ is omitted in Eq. (42), since the coefficients $[C_L^{\mathrm{NP}}]_{ij}$ and $[L_{\nu d}^{V,LL}]_{ij23}^{\mathrm{NP}}$ have no scale dependence. Let us consider the coefficients for the $b \to s\mu^+\mu^-$ transition. The coefficients $[C_{9V}^{\mathrm{NP}}(\mu)]_{22}$ and $[C_{10A}^{\mathrm{NP}}(\mu)]_{22}$ in Eqs. (40) and (41) are dominated by the LEFT coefficient $[L_{ed}^{V,LL}(\mu)]_{2223}$ generated at the tree level, while the contributions from $[L_{de}^{V,LR}(\mu)]_{3222}$ induced at the one-loop level are subdominant. Hence, the approximate relation $[C_{9V}^{\mathrm{NP}}(\mu)]_{22} \approx -[C_{10A}^{\mathrm{NP}}(\mu)]_{22}$ holds in the current model [38].

D. Constraints

In the current model, the S_3 leptoquark has sizable couplings to quarks and leptons in the second and third generations. Strong constraints on the parameter space of the model come from the mass difference of B_s and $\bar{B}_s$ mesons denoted by ΔM_s, the branching ratios for the $B \to K^{(*)}\nu\bar{\nu}$ decays, the LFUV tests in the $B \to K^{(*)}\ell^+\ell^-$ ($\ell = e, \mu$) decays, and the branching ratio for the $B_s \to \mu^+\mu^-$ decay. NP contributions to ΔM_s are generated at the one-loop level, while those to the others are at the tree level. The current experimental data for these observables are summarized in Table III together with other relevant observables. For the $B \to K^{(*)}\ell^+\ell^-$ decays, we do not consider their branching ratios and the angular observables

TABLE III. Current measurements and future experimental sensitivities of flavor observables. The first column represents the corresponding transition, and the second column shows the dominant coupling that induces the transition, where Loop denotes a loop-level transition.

Transition	Couplings	Observable	Current measurement	Future sensitivity
$b \to s\mu^+\mu^-$	$(\bar{Y}_3^{QL*})_{22}(\bar{Y}_3^{QL})_{32}$	$R_{K^+}[0.1, 1.1]$	$0.994^{+0.090+0.029}_{-0.082-0.027}$ [78,79]	
		$R_{K^{*0}}[0.1, 1.1]$	$0.927^{+0.093+0.036}_{-0.087-0.035}$ [78,79]	
		$R_{K^+}[1.1, 6.0]$	$0.949^{+0.042+0.022}_{-0.041-0.022}$ [78,79]	± 0.007 [80]
		$R_{K^{*0}}[1.1, 6.0]$	$1.027^{+0.072+0.027}_{-0.068-0.026}$ [78,79]	± 0.008 [80]
		$\mathcal{B}(B_s \to \mu^+\mu^-)$	$(3.01 \pm 0.35) \times 10^{-9}$ [81]	$\pm 0.16 \times 10^{-9}$ [80]
Loop	$(\bar{Y}_3^{QL*})_{23}(\bar{Y}_3^{QL})_{33}$	ΔM_s	(17.765 ± 0.006) ps^{-1} [81]	
$b \to s\nu\bar{\nu}$	$(\bar{Y}_3^{QL*})_{23}(\bar{Y}_3^{QL})_{33}$	$\mathcal{B}(B^+ \to K^+\nu\bar{\nu})$	$< 1.6 \times 10^{-5}$ (90%) [82]	± 11 % of SM [83]
		$\mathcal{B}(B^0 \to K_S\nu\bar{\nu})$	$< 1.3 \times 10^{-5}$ (90%)[84]	
		$\mathcal{B}(B^+ \to K^{*+}\nu\bar{\nu})$	$< 4.0 \times 10^{-5}$ (90%) [85]	± 9.3 % of SM [83]
		$\mathcal{B}(B^0 \to K^{*0}\nu\bar{\nu})$	$< 1.8 \times 10^{-5}$ (90%) [84]	± 9.6 % of SM [83]
$b \to c\tau^-\bar{\nu}$	$(\bar{Y}_3^{QL*})_{23}(\bar{Y}_3^{QL})_{33}$	$R(D)$	0.357 ± 0.029 [86]	$(\pm 2.0 \pm 2.5)$% [83]
		$R(D^*)$	0.284 ± 0.012 [86]	$(\pm 1.0 \pm 2.0)$% [83]
$b \to s\tau^+\tau^-$	$(\bar{Y}_3^{QL*})_{23}(\bar{Y}_3^{QL})_{33}$	$\mathcal{B}(B_s \to \tau^+\tau^-)$	$< 5.2 \times 10^{-3}$ (90%) [87]	5×10^{-4} [80]
		$\mathcal{B}(B^+ \to K^+\tau^+\tau^-)$	$< 2.25 \times 10^{-3}$ (90%) [88]	2.0×10^{-5} [83]
		$\mathcal{B}(B^0 \to K^{*0}\tau^+\tau^-)$	$< 3.1 \times 10^{-3}$ (90%) [89]	5.3×10^{-4} [90]
$b \to s\mu^+\tau^-$	$(\bar{Y}_3^{QL})^*_{23}(\bar{Y}_3^{QL})_{32}$	$\mathcal{B}(B_s \to \mu^\mp\tau^\pm)$	$< 3.4 \times 10^{-5}$ (90%) [91]	3×10^{-6} [80]
		$\mathcal{B}(B^+ \to K^+\mu^-\tau^+)$	$< 5.9 \times 10^{-6}$ (90%) [92]	3.3×10^{-6} [83]
		$\mathcal{B}(B^0 \to K^{*0}\mu^-\tau^+)$	$< 1.0 \times 10^{-5}$ (90%) [93]	
$b \to s\mu^-\tau^+$	$(\bar{Y}_3^{QL})^*_{22}(\bar{Y}_3^{QL})_{33}$	$\mathcal{B}(B^+ \to K^+\mu^+\tau^-)$	$< 2.45 \times 10^{-5}$ (90%) [92]	3.3×10^{-6} [83]
		$\mathcal{B}(B^0 \to K^{*0}\mu^+\tau^-)$	$< 8.2 \times 10^{-6}$ (90%) [93]	
$\tau^- \to \mu^-\bar{s}s$	$(\bar{Y}_3^{QL})^*_{22}(\bar{Y}_3^{QL})_{23}$	$\mathcal{B}(\tau^- \to \mu^-\phi)$	$< 2.3 \times 10^{-8}$ (90%) [94]	8.4×10^{-10} [95]
$b\bar{b} \to \mu^\pm\tau^\mp$	$(\bar{Y}_3^{QL*})_{32}(\bar{Y}_3^{QL})_{33}$	$\mathcal{B}(\Upsilon(1S) \to \mu^\pm\tau^\mp)$	$< 2.7 \times 10^{-6}$ (90%) [96]	
		$\mathcal{B}(\Upsilon(2S) \to \mu^\pm\tau^\mp)$	$< 3.3 \times 10^{-6}$ (90%) [97]	
		$\mathcal{B}(\Upsilon(3S) \to \mu^\pm\tau^\mp)$	$< 3.1 \times 10^{-6}$ (90%) [97]	
Loop	$(\bar{Y}_3^{QL*})_{32}(\bar{Y}_3^{QL})_{33}$	$\mathcal{B}(\tau^- \to \mu^-\gamma)$	$< 4.2 \times 10^{-8}$ (90%) [98]	6.9×10^{-9} [95]
		$\mathcal{B}(\tau^- \to \mu^-\mu^+\mu^-)$	$< 2.1 \times 10^{-8}$ (90%) [99]	3.6×10^{-10} [95]
		$\mathcal{B}(Z \to \mu^\mp\tau^\pm)$	$< 6.5 \times 10^{-6}$ (95%) [100]	$\mathcal{O}(10^{-9})$ [101]

that exhibit some tensions with the SM [71], since they suffer from hadronic uncertainties [72–77].

For the mass difference ΔM_s, we utilize the following formula that is normalized to the SM value:

$$\frac{\Delta M_s}{\Delta M_s^{\rm SM}} = \left|1 + \frac{C_{bs}^{LL,\rm NP}(m_b)}{R_{\rm SM}^{\rm loop}}\right|,$$
$$C_{bs}^{LL,\rm NP}(m_b) = -\frac{\sqrt{2}}{4G_F(V_{tb}V_{ts}^*)^2}\,[L_{dd}^{V,LL}(m_b)]_{2323}^{\rm NP}, \quad (43)$$

where the SM loop contribution $R_{\rm SM}^{\rm loop} = (1.310 \pm 0.010) \times 10^{-3}$ and the SM prediction $\Delta M_s^{\rm SM} = (18.4^{+0.7}_{-1.2})$ ps^{-1} are evaluated in Ref. [45]. Our analysis includes the theoretical uncertainty in $\Delta M_s^{\rm SM}$, which is much larger than the experimental one. In the current model, the LEFT coefficient $[L_{dd}^{V,LL}(m_b)]_{2323}^{\rm NP}$, given in Eq. (D10), is generated at the one-loop level. Contributions from other coefficients with the right-handed quarks are suppressed by the small quark masses and neglected here. We use the PDG average of the measurements for ΔM_s [81], which gives a constraint on the product of the S_3 Yukawa couplings $(\bar{Y}_3^{QL}\bar{Y}_3^{QL\dagger})_{32}$. Because of the hierarchy in the magnitudes of the couplings, the product is dominated by $(\bar{Y}_3^{QL})^*_{23}(\bar{Y}_3^{QL})_{33}$ compared with $(\bar{Y}_3^{QL})^*_{21}(\bar{Y}_3^{QL})_{31}$ and $(\bar{Y}_3^{QL})^*_{22}(\bar{Y}_3^{QL})_{32}$.

The product $(\bar{Y}_3^{QL}\bar{Y}_3^{QL\dagger})_{32}$ is also constrained from the branching ratios for $B \to K^{(*)}\nu\bar{\nu}$, which are calculated as

$$\frac{\mathcal{B}(B \to K^{(*)}\nu\bar{\nu})}{\mathcal{B}(B \to K^{(*)}\nu\bar{\nu})_{\rm SM}} = \frac{1}{3}\sum_{ij}\frac{|C_L^{\rm SM}\delta_{ij} + [C_L^{\rm NP}]_{ij}|^2}{|C_L^{\rm SM}|^2}, \quad (44)$$

where the SM coefficient is given by $C_L^{\rm SM} = -X_t/s_W^2$ with $X_t = 1.469$ and $s_W^2 = 1 - c_W^2$, and the SM predictions

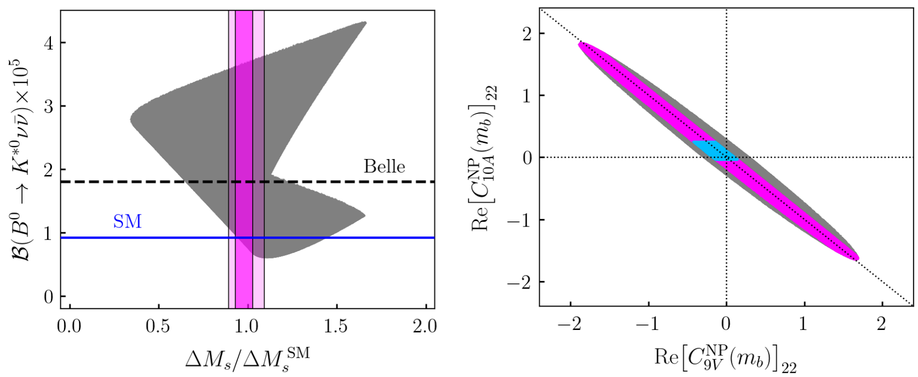

FIG. 4. Left: constraints from $\Delta M_s/\Delta M_s^{\rm SM}$ and $\mathcal{B}(B^0 \to K^{*0}\nu\bar{\nu})$. The gray region represents the predictions which are consistent with the low-energy values of the gauge couplings and the fermion masses and mixing. The vertical bands in magenta correspond to the experimental measurements at the one and two sigma ranges, and the horizontal lines are the 90% upper limit at Belle (black dashed line) and the SM prediction (blue solid line). Right: constraints on $\mathrm{Re}[(C_{9V}^{\rm NP})_{22}]$ and $\mathrm{Re}[(C_{10A}^{\rm NP})_{22}]$ at the m_b scale, where the oblique dotted line represents $\mathrm{Re}[(C_{9V}^{\rm NP})_{22}] = -\mathrm{Re}[(C_{10A}^{\rm NP})_{22}]$. The magenta region can satisfy the experimental bounds from ΔM_s and $\mathcal{B}(B^0 \to K^{*0}\nu\bar{\nu})$, while the cyan region can satisfy further with $R_{K^+}[1.1, 6.0]$, $R_{K^{*0}}[1.1, 6.0]$, and $\mathcal{B}(B_s \to \mu^+\mu^-)$. These regions are overlaid on top of the gray one, which corresponds to that in the left plot.

are $\mathcal{B}(B^+ \to K^+\nu\bar{\nu})_{\rm SM} = (3.98 \pm 0.43 \pm 0.19) \times 10^{-6}$, $\mathcal{B}(B^0 \to K^0\nu\bar{\nu})_{\rm SM} = (\tau_{B^0}/\tau_{B^+})\mathcal{B}(B^+ \to K^+\nu\bar{\nu})_{\rm SM}$, $\mathcal{B}(B^0 \to K^{*0}\nu\bar{\nu})_{\rm SM} = (9.19 \pm 0.86 \pm 0.50) \times 10^{-6}$, and $\mathcal{B}(B^+ \to K^{*+}\nu\bar{\nu})_{\rm SM} = (\tau_{B^+}/\tau_{B^0})\mathcal{B}(B^0 \to K^{*0}\nu\bar{\nu})_{\rm SM}$ with τ_{B^+} and τ_{B^0} being the lifetimes of B mesons [102]. The NP contribution $C_L^{\rm NP}$ is defined by Eq. (42), where the one-loop expression of the LEFT coefficient $[L_{\nu d}^{V,LL}]_{ij23}^{\rm NP}$ is given in Eq. (D3). We select $B^0 \to K^{*0}\nu\bar{\nu}$ as a representative of the $B \to K^{(*)}\nu\bar{\nu}$ processes in our numerical analysis, where the use of the other processes gives similar results.[3] The upper limit on $\mathcal{B}(B^0 \to K^{*0}\nu\bar{\nu})$ is reported from the Belle experiment [84], and provides a constraint on $(\bar{Y}_3^{QL})^*_{23}(\bar{Y}_3^{QL})_{33}$.

In the left plot of Fig. 4, we present constraints in the plane of $\Delta M_s/\Delta M_s^{\rm SM}$ and $\mathcal{B}(B^0 \to K^{*0}\nu\bar{\nu})$, where the gray region is obtained with the model parameters that are consistent with the low-energy values of the gauge couplings, the fermion masses, and the CKM matrix elements. Here and hereafter, we take $m_{S_3} = 2$ TeV and $\cot\theta_H = 50$ as well as the input parameters in Table II. A large portion of the parameter space is excluded by the measurement of ΔM_s (magenta vertical bands) [81] and by the upper limit for $\mathcal{B}(B^0 \to K^{*0}\nu\bar{\nu})$ (black horizontal dashed line) [84], where the two bands for ΔM_s correspond to the one-sigma and two-sigma regions.

Moreover, the measurements for the $b \to s\mu^+\mu^-$ processes listed in Table III provide constraints on the product of the Yukawa couplings $(\bar{Y}_3^{QL*})_{22}(\bar{Y}_3^{QL})_{32}$. In particular, experimental searches for the violation of the lepton-flavor-universality (LFU) in $b \to s$ semileptonic decays provide severe constraints on our scenario. The LFU ratios R_H ($H = K^+, K^{*0}$) are defined by

$$R_H[q^2_{\rm min}, q^2_{\rm max}] = \frac{\int_{q^2_{\rm min}}^{q^2_{\rm max}} dq^2 \frac{d\mathcal{B}(B\to H\mu^+\mu^-)}{dq^2}}{\int_{q^2_{\rm min}}^{q^2_{\rm max}} dq^2 \frac{d\mathcal{B}(B\to He^+e^-)}{dq^2}}, \tag{45}$$

where $q^2_{\rm min}$ and $q^2_{\rm max}$ are given in units of GeV^2. For example, approximate formulas for the region of 1.1 GeV$^2 < q^2 < 6.0$ GeV^2 are given in Ref. [104]:

$$R_K[1.1, 6.0] \approx 1.00 + 0.23\mathrm{Re}(\Delta C_{9V}^{\rm NP}) - 0.25\mathrm{Re}(\Delta C_{10A}^{\rm NP}), \tag{46}$$

$$R_{K^*}[1.1, 6.0] \approx 1.00 + 0.20\mathrm{Re}(\Delta C_{9V}^{\rm NP}) - 0.27\mathrm{Re}(\Delta C_{10A}^{\rm NP}), \tag{47}$$

where $\Delta C_{9V}^{\rm NP} \equiv [C_{9V}^{\rm NP}(m_b)]_{22} - [C_{9V}^{\rm NP}(m_b)]_{11}$ and $\Delta C_{10A}^{\rm NP} \equiv [C_{10A}^{\rm NP}(m_b)]_{22} - [C_{10A}^{\rm NP}(m_b)]_{11}$. These LFU ratios are calculated very accurately in the SM, where the hadronic uncertainty is highly canceled by considering the ratios [105], and the QED correction provides a positive contribution to the ratios about less than 3% for 1 GeV$^2 < q^2 < 6$ GeV^2 [106,107]. The above approximate formulas are derived by neglecting the QED corrections. The theoretical uncertainties are negligible in our study. The recent measurements at LHCb [79] listed in Table III are compatible with the SM predictions. We adopt only $R_K[1.1, 6.0]$ and $R_{K^*}[1.1, 6.0]$ as constraints, since the ratios in the low q^2 regions $R_K[0.1, 1.1]$ and $R_{K^*}[0.1, 1.1]$ have larger experimental uncertainties. In addition, we also

[3] Very recently the Belle II collaboration has reported the first evidence of the $B^+ \to K^+\nu\bar{\nu}$ decay as $\mathcal{B}(B^+ \to K^+\nu\bar{\nu}) = (2.4 \pm 0.5^{+0.5}_{-0.4}) \times 10^{-5}$ [103]. We do not take into account it in our analysis.

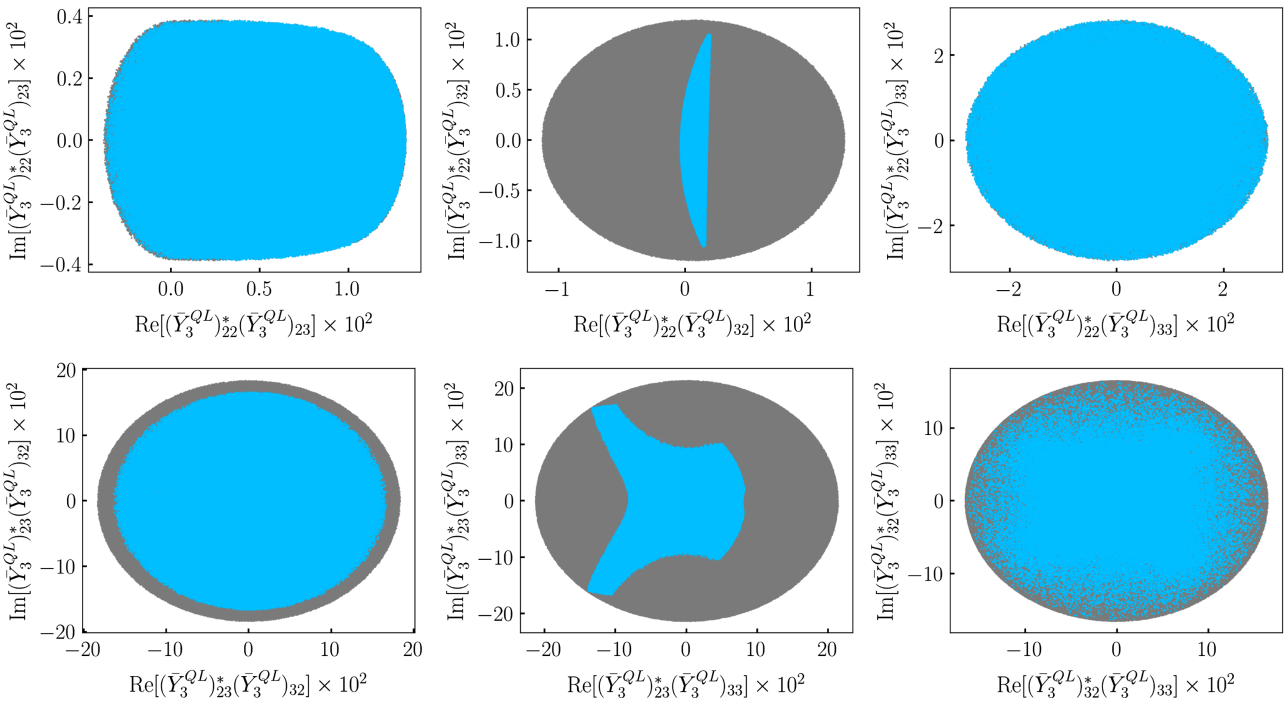

FIG. 5. Allowed region for the products of the Yukawa couplings of the S_3 leptoquark at the S_3 mass scale, where the cyan region shows the parameter points that are consistent with ΔM_s, $R_{K^+}[1.1, 6.0]$, $R_{K^{*0}}[1.1, 6.0]$, and $\mathcal{B}(B_s \to \mu^+\mu^-)$ within two sigma and $\mathcal{B}(B^0 \to K^{*0}\nu\bar{\nu})$ at 90% CL. The cyan regions are overlaid on top of the gray ones, which correspond to those in Fig. 4.

consider the branching ratio for the leptonic decay $B_s \to \mu^+\mu^-$, which is written simply with the NP contribution to C_{10A}:

$$\mathcal{B}(B_s \to \mu^+\mu^-) = \mathcal{B}(B_s \to \mu^+\mu^-)_{\mathrm{SM}} \left| 1 + \frac{[C_{10A}^{\mathrm{NP}}(m_b)]_{22}}{C_{10A}^{\mathrm{SM}}(m_b)} \right|^2, \tag{48}$$

where the SM values are $\mathcal{B}(B_s \to \mu^+\mu^-)_{\mathrm{SM}} = (3.65 \pm 0.23) \times 10^{-9}$ [108] and $C_{10A}^{\mathrm{SM}}(m_b) = -4.2$ [109]. It is noted that a nonvanishing decay width difference $\Delta\Gamma_s$ of the B_s system has to be taken into account when comparing the theoretical value calculated using Eq. (48) with the experimental data in Table III, since the time dependence of the decay rate is integrated in the experiment [110,111]. This gives only a minor effect on our numerical analysis. In the current model, $[C_{9V}^{\mathrm{NP}}(m_b)]_{22}$ and $[C_{10A}^{\mathrm{NP}}(m_b)]_{22}$ appearing in $R_K[1.1, 6.0]$, $R_{K^*}[1.1, 6.0]$, and $\mathcal{B}(B_s \to \mu^+\mu^-)$ are dominated by the LEFT coefficient $[L_{ed}^{V,LL}(m_b)]_{2223}$, which is given in terms of the product of the S_3 Yukawa couplings $(\bar{Y}_3^{QL*})_{22}(\bar{Y}_3^{QL})_{32}$ at the tree level.

The right plot of Fig. 4 shows constraints on $\mathrm{Re}[C_{9V}^{\mathrm{NP}}(m_b)]_{22}$ and $\mathrm{Re}[C_{10A}^{\mathrm{NP}}(m_b)]_{22}$. The magenta region can satisfy the experimental bounds from ΔM_s within two sigma and $\mathcal{B}(B^0 \to K^{*0}\nu\bar{\nu})$ at 90% confidence level (CL), while the cyan region can satisfy further $R_{K^+}[1.1, 6.0]$, $R_{K^{*0}}[1.1, 6.0]$, and $\mathcal{B}(B_s \to \mu^+\mu^-)$ within two sigma. These regions are overlaid on top of the gray one, which corresponds to that in the left plot.

We also present allowed regions for the products of the S_3 Yukawa couplings at the S_3 mass scale in Fig. 5. Here the cyan regions show the parameter points that are consistent with ΔM_s, $R_{K^+}[1.1, 6.0]$, $R_{K^{*0}}[1.1, 6.0]$, and $\mathcal{B}(B_s \to \mu^+\mu^-)$ within two sigma and $\mathcal{B}(B^0 \to K^{*0}\nu\bar{\nu})$ at 90% CL. It is noted that the cyan regions are overlaid on top of the gray regions that correspond to those in Fig. 4. The magnitudes of the products in the upper row of Fig. 5 are smaller than those in the lower row because of the hierarchy given in Eq. (31). The product $(\bar{Y}_3^{QL*})_{22}(\bar{Y}_3^{QL})_{32}$ is highly constrained by $R_{K^+}[1.1, 6.0]$, $R_{K^{*0}}[1.1, 6.0]$, and $\mathcal{B}(B_s \to \mu^+\mu^-)$, while $(\bar{Y}_3^{QL*})_{23}(\bar{Y}_3^{QL})_{33}$ is by ΔM_s and $\mathcal{B}(B^0 \to K^{*0}\nu\bar{\nu})$. The other products are less constrained by these observables.

E. Predictions

The S_3 leptoquark can generate various LFV and LFUV with the second- and third-generation fermions. Under the constraints studied in Sec. III D, we here consider the following observables: $R(D^{(*)})$, $\mathcal{B}(B_s \to \tau^+\tau^-)$, $\mathcal{B}(B_s \to \mu^\mp\tau^\pm)$, $\mathcal{B}(B \to K^{(*)}\mu^\mp\tau^\pm)$, $\mathcal{B}(\Upsilon(nS) \to \mu^\pm\tau^\mp)$, $\mathcal{B}(\tau^- \to \mu^-\phi)$, $\mathcal{B}(\tau^- \to \mu^-\gamma)$, $\mathcal{B}(\tau^- \to \mu^-\mu^+\mu^-)$, and $\mathcal{B}(Z \to \mu^\mp\tau^\pm)$. The first six observables receive tree-level contributions, while the rest are induced at the one-loop level. Figures 6 and 7 show predictions for these observables in the current model. Here we only consider

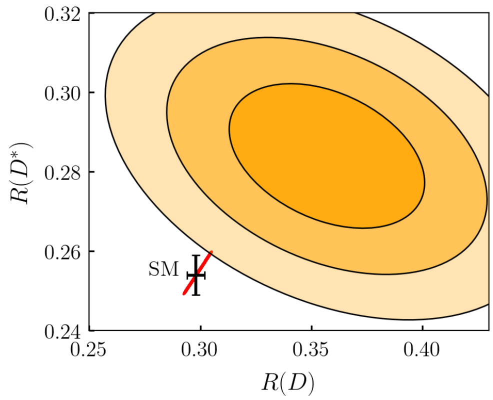

FIG. 6. Predictions for $R(D)$ and $R(D^*)$ (denoted by the red points) with the HFLAV average of their experimental measurements at the levels of one sigma, two sigma, and three sigma (denoted by the orange ellipses) and the SM values (denoted by the black cross). Theoretical uncertainties associated with the SM errors are not included in the predictions.

flavor-changing-neutral-current processes except for $R(D^{(*)})$, since the S_3 effects on charged-current processes, such as $B^0 \to D^{(*)-}\mu^+\nu$ and $D_s^+ \to \mu^+\nu$, are not significant.

In Fig. 6, we present the predictions for the ratios $R(D^{(*)}) = \mathcal{B}(B^0 \to D^{(*)}\tau^+\nu)/\mathcal{B}(B^0 \to D^{(*)}\ell^+\nu)$ for $\ell = e, \mu$ calculated under the constraints from $\Delta M_s/\Delta M_s^{\rm SM}$, $\mathcal{B}(B^0 \to K^{*0}\nu\bar{\nu})$, $R_{K^+}[1.1, 6.0]$, $R_{K^{*0}}[1.1, 6.0]$, and $\mathcal{B}(B_s \to \mu^+\mu^-)$. At the tree level $R(D^{(*)})$ are given by

$$R(D^{(*)}) \approx R(D^{(*)})_{\rm SM}(1 + 2{\rm Re}[C_{V_1}^{\rm NP}(m_b)]_{33}), \quad (49)$$

where we adopt the SM predictions $R(D)_{\rm SM} = 0.298 \pm 0.004$ and $R(D^*)_{\rm SM} = 0.254 \pm 0.005$ [86]. The coefficient $C_{V_1}^{\rm NP}$ is defined through the effective Lagrangian,

$$\mathcal{L}_{\rm eff} = -\frac{4G_F}{\sqrt{2}} V_{cb}^* (\delta_{ij} + [C_{V_1}^{\rm NP}(m_b)]_{ij})(\bar{\hat{b}}_L\gamma^\mu \hat{c}_L)(\bar{\nu}_{Li}\gamma_\mu \hat{e}_{Lj}),$$

$$[C_{V_1}^{\rm NP}(m_b)]_{33} = -\frac{1}{2\sqrt{2}G_F V_{cb}^*}[L_{\nu edu}^{V,LL}(m_b)]_{3332}^{\rm NP}, \quad (50)$$

where we use the tree-level result for the LEFT coefficient $[L_{\nu edu}^{V,LL}(m_b)]_{3332}^{\rm NP}$ given in Eq. (36). We keep only the 33 component of $C_{V_1}^{\rm NP}$ in Eq. (49), since the dominant NP contributions arise in the 23, 32, and 33 ones in the current model and only the 33 one has an interference with the SM contribution. We use the average of the experimental data by the Heavy Flavor Averaging Group (HFLAV) [86]. Here the $b \to c\tau^-\bar{\nu}$ transition is dominated by the contribution from the product $(\bar{Y}_3^{QL})_{23}^*(\bar{Y}_3^{QL})_{33}$, which also contributes to $b \to s\nu\bar{\nu}$ and ΔM_s. It is known that the S_3 contribution that explains the $b \to c$ anomaly is severely constrained by the $b \to s\nu\bar{\nu}$ processes and ΔM_s [40]. Consequently, the S_3 contribution does not alter $R(D^{(*)})$ significantly, and thus the resolution of the $R(D^{(*)})$ anomaly requires an extension of the model [112,113]. We do not consider such a possibility in the current paper.

Next, let us consider decay processes involving $b \to s\tau^+\tau^-$ transition. The studies of NP contributions to this transition are found, for example, in Refs. [114,115]. In the current model, the contributions to the $b \to s\tau^+\tau^-$ leptonic and semileptonic decays arise at the tree level through the product $(\bar{Y}_3^{QL})_{23}^*(\bar{Y}_3^{QL})_{33}$. As in the case of $B_s \to \mu^+\mu^-$ in Eq. (48), the leptonic mode receives NP contribution to C_{10A}:

$$\mathcal{B}(B_s \to \tau^+\tau^-) = \mathcal{B}(B_s \to \tau^+\tau^-)_{\rm SM}\left|1 + \frac{[C_{10A}^{\rm NP}(m_b)]_{33}}{C_{10A}^{\rm SM}(m_b)}\right|^2, \quad (51)$$

where the SM prediction is $\mathcal{B}(B_s \to \tau^+\tau^-)_{\rm SM} = (7.73 \pm 0.49) \times 10^{-7}$ [108]. Moreover, the branching ratios of the semileptonic modes in the large q^2 region are calculated in Ref. [115]:

$$\begin{aligned}\mathcal{B}(B \to K\tau^+\tau^-)^{[15,22]} &= 10^{-7}(1.20 + 0.15{\rm Re}[C_{9V}^{\rm NP}(m_b)]_{33} \\ &\quad - 0.42{\rm Re}[C_{10A}^{\rm NP}(m_b)]_{33} + 0.02|[C_{9V}^{\rm NP}(m_b)]_{33}|^2 \\ &\quad + 0.05|[C_{10A}^{\rm NP}(m_b)]_{33}|^2), \end{aligned} \quad (52)$$

$$\begin{aligned}\mathcal{B}(B \to K^*\tau^+\tau^-)^{[15,19]} &= 10^{-7}(0.98 + 0.38{\rm Re}[C_{9V}^{\rm NP}(m_b)]_{33} - 0.14{\rm Re}[C_{10A}^{\rm NP}(m_b)]_{33} \\ &\quad + 0.05|[C_{9V}^{\rm NP}(m_b)]_{33}|^2 + 0.02|[C_{10A}^{\rm NP}(m_b)]_{33}|^2), \end{aligned} \quad (53)$$

which are the averages of the charged and the neutral modes. The predicted branching ratios in the SM are of $\mathcal{O}(10^{-7})$ [115]. The branching ratios for these leptonic and semileptonic modes can largely deviate from their SM values. Figure 7(a) shows that $\mathcal{B}(B_s \to \tau^+\tau^-)$ can be as large as $\mathcal{O}(10^{-5})$, which is an order of magnitude smaller than the future sensitivity at LHCb with 300 fb^{-1} [80]. Similarly, the predictions for $\mathcal{B}(B \to K^{(*)}\tau^+\tau^-)$ in the large q^2 region can be enhanced by an order of magnitude, but it is still much smaller than the future sensitivity at Belle II with 50 fb^{-1} [83].

We also study the LFV processes $b \to s\mu^+\tau^-$ and $b \to s\mu^-\tau^+$, which are generated through the products of the S_3 Yukawa couplings $(\bar{Y}_3^{QL})_{23}^*(\bar{Y}_3^{QL})_{32}$ and $(\bar{Y}_3^{QL})_{22}^*(\bar{Y}_3^{QL})_{33}$, respectively. Because of the hierarchy in the magnitudes of the S_3 Yukawa couplings presented in Eq. (31) and Fig. 5, the relation $|(\bar{Y}_3^{QL})_{23}^*(\bar{Y}_3^{QL})_{32}| \gg |(\bar{Y}_3^{QL})_{22}^*(\bar{Y}_3^{QL})_{33}|$ holds typically. At the LHC experiments, the branching ratio for the leptonic decay is measured as a sum of the two channels $B_s \to \mu^-\tau^+$ and $B_s \to \mu^+\tau^-$. The corresponding theoretical formula is given by [116]

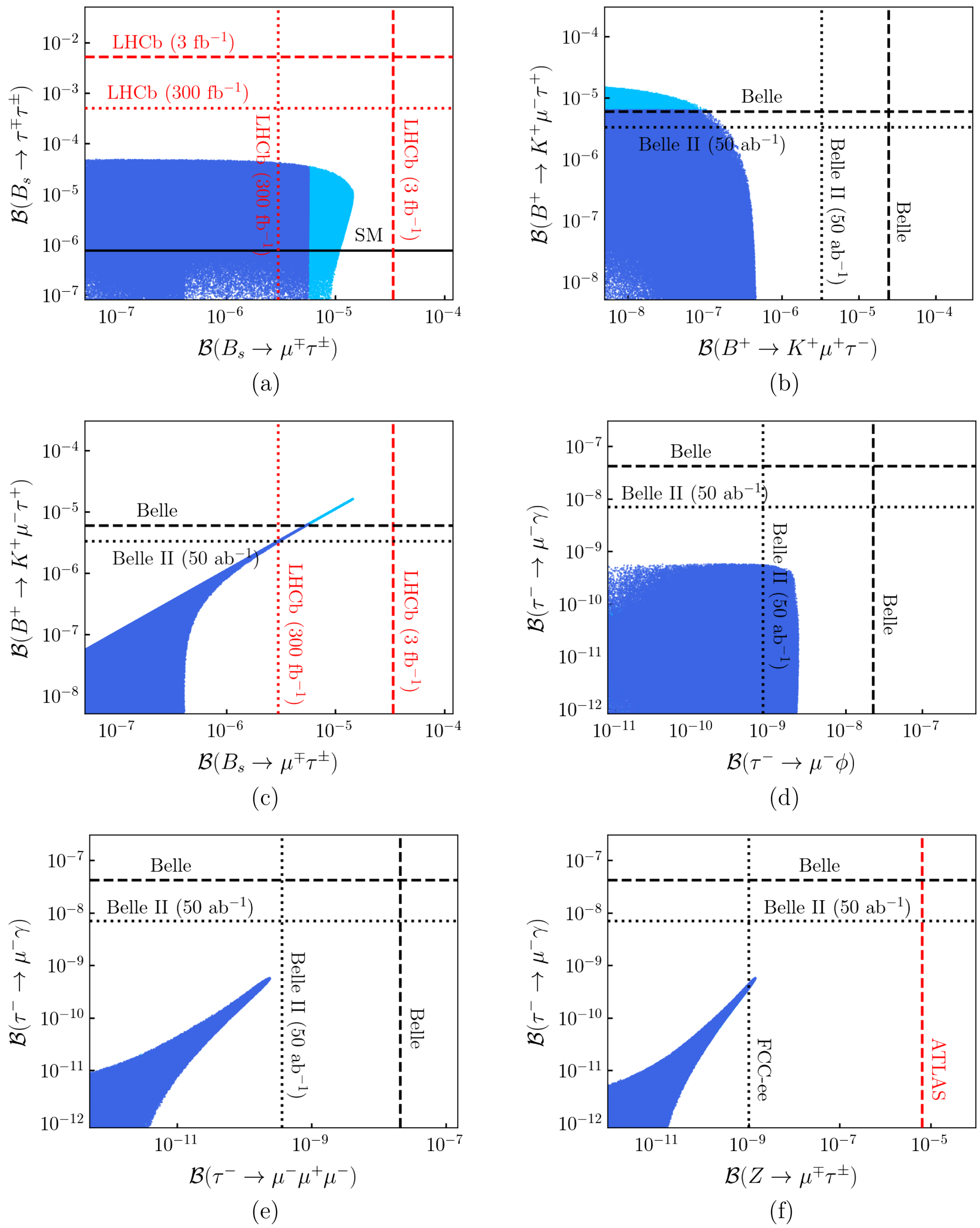

FIG. 7. Predictions on relevant flavor processes, where the colored regions satisfy the experimental bounds from $R_{K^+}[1.1, 6.0]$, $R_{K^{*0}}[1.1, 6.0]$, $\mathcal{B}(B_s \to \mu^+\mu^-)$, and ΔM_s within two sigma and $\mathcal{B}(B^0 \to K^{*0}\nu\bar{\nu})$ at 90% CL. The red and black dashed lines show the present upper bound on each processes by LHC experiments and B factories, respectively, and the red and black dotted lines show the sensitivities expected at the LHCb with 300 fb^{-1} and the e^+e^- experiments (such as the Belle II with 50 ab^{-1} and FCC-ee), respectively. The cyan regions in (a), (b), and (c) are excluded by the upper limit on $\mathcal{B}(B^+ \to K^+\mu^-\tau^+)$ at Belle.

$$\begin{aligned}\mathcal{B}(B_s \to \mu^\mp\tau^\pm) &= \mathcal{B}(B_s \to \mu^-\tau^+) + \mathcal{B}(B_s \to \mu^+\tau^-),\\ &= \frac{\tau_{B_s} f_{B_s}^2 m_{B_s} m_\tau^2 \alpha^2 G_F^2 |V_{ts}^* V_{tb}|^2}{64\pi^3}\left(1 - \frac{m_\tau^2}{m_{B_s}^2}\right)^2\\ &\quad\times\left(|[C_{9V}^{\mathrm{NP}}(m_b)]_{23}|^2 + |[C_{10A}^{\mathrm{NP}}(m_b)]_{23}|^2 + |[C_{9V}^{\mathrm{NP}}(m_b)]_{32}|^2 + |[C_{10A}^{\mathrm{NP}}(m_b)]_{32}|^2\right),\end{aligned} \tag{54}$$

where m_τ and τ_τ are the mass and the lifetime of τ lepton; m_{B_s}, τ_{B_s}, and f_{B_s} are the mass, the lifetime, and the decay constant of B_s meson; and the muon mass is neglected. As shown in Fig. 7(a), the prediction on $\mathcal{B}(B_s \to \mu^\mp\tau^\pm)$ can be as large as $\mathcal{O}(10^{-5})$, which may be probed by the LHCb measurement with 300 fb^{-1} [80]. For the semileptonic channels, approximate numerical formulas are given by [117]

$$\mathcal{B}(B^+ \to K^+\mu^-\tau^+) = 10^{-9}\left(12.5|[C_{9V}^{\rm NP}(m_b)]_{32}|^2 + 12.9|[C_{10A}^{\rm NP}(m_b)]_{32}|^2\right)\frac{\tau_{B^+}}{\tau_{B^0}}, \tag{55}$$

$$\mathcal{B}(B^+ \to K^+\mu^+\tau^-) = 10^{-9}\left(12.5|[C_{9V}^{\rm NP}(m_b)]_{23}|^2 + 12.9|[C_{10A}^{\rm NP}(m_b)]_{23}|^2\right)\frac{\tau_{B^+}}{\tau_{B^0}}, \tag{56}$$

$$\mathcal{B}(B^0 \to K^{*0}\mu^-\tau^+) = 10^{-9}\left(22.1|[C_{9V}^{\rm NP}(m_b)]_{32}|^2 + 20.6|[C_{10A}^{\rm NP}(m_b)]_{32}|^2\right), \tag{57}$$

$$\mathcal{B}(B^0 \to K^{*0}\mu^+\tau^-) = 10^{-9}\left(22.1|[C_{9V}^{\rm NP}(m_b)]_{23}|^2 + 20.6|[C_{10A}^{\rm NP}(m_b)]_{23}|^2\right). \tag{58}$$

It is noted that $B^+ \to K^+\mu^-\tau^+$ ($B^0 \to K^{*0}\mu^-\tau^+$) and $B^+ \to K^+\mu^+\tau^-$ ($B^0 \to K^{*0}\mu^+\tau^-$) receive contributions from $|(\bar{Y}_3^{QL})^*_{23}(\bar{Y}_3^{QL})_{32}|$ and $|(\bar{Y}_3^{QL})^*_{22}(\bar{Y}_3^{QL})_{33}|$, respectively. We here present results on $B^+ \to K^+\mu^\mp\tau^\pm$, since future sensitivities at Belle II can be found for these processes in Ref. [83]. As shown in Fig. 7(b), $\mathcal{B}(B^+ \to K^+\mu^-\tau^+)$ can be large enough to be observed at Belle II with 50 ab^{-1}, while $\mathcal{B}(B^+ \to K^+\mu^+\tau^-)$ is out of the reach of Belle II. A part of the parameter space is already excluded by the current measurement of $\mathcal{B}(B^+ \to K^+\mu^-\tau^+)$ at Belle, but it does not alter the other predictions in Fig. 7 except for that of $\mathcal{B}(B_s \to \mu^\mp\tau^\pm)$. Figure 7(c) shows a strong correlation between $\mathcal{B}(B_s \to \mu^\mp\tau^\pm)$ and $\mathcal{B}(B^+ \to K^+\mu^-\tau^+)$, since both of them are induced mainly by $|(\bar{Y}_3^{QL})^*_{23}(\bar{Y}_3^{QL})_{32}|$. The current upper limit on $\mathcal{B}(B^+ \to K^+\mu^-\tau^+)$ directly leads to the limit on $\mathcal{B}(B_s \to \mu^\mp\tau^\pm)$. These correlations among the $b \to s\mu^+\tau^-$ and $b \to s\mu^-\tau^+$ observables can be explored by the combination of the Belle II and the LHCb measurements.

Besides, we consider the LFV decays of heavy quarkonia, $\Upsilon(nS) \to \mu^\mp\tau^\pm$ ($n = 1, 2, 3$). The branching ratios for these processes are given by [118–120]

$$\mathcal{B}(\Upsilon(nS) \to \mu^\pm\tau^\mp) = \mathcal{B}(\Upsilon(nS) \to e^+e^-)_{\rm SM}\frac{1}{2}\left|\frac{3m_{\Upsilon(nS)}^2\left[L_{ed}^{V,LL}(m_{\Upsilon(nS)})\right]_{2333}}{8\pi\alpha}\right|^2, \tag{59}$$

where $m_{\Upsilon(nS)}$ is the mass of $\Upsilon(nS)$, and the charged-lepton masses are neglected. From the bottom-right plot in Fig. 5, we estimate the magnitude of the LEFT coupling as $|[L_{ed}^{V,LL}(m_{\Upsilon(nS)})]_{2333}| \sim |(\bar{Y}_3^{QL*})_{32}(\bar{Y}_3^{QL})_{33}|/m_{S_3}^2 \lesssim \mathcal{O}(10^{-8}\ \mathrm{GeV}^2)$. Therefore, the branching ratios are as large as $\mathcal{O}(10^{-11})$, which are too small to be measured at current and near-future experiments.

Furthermore, the S_3 leptoquark contributions also induce LFV decays of tau lepton. At the tree level, the $\tau^- \to \mu^-\phi$ decay with $\tau^- \to \mu^-\bar{s}s$ transition is generated through the S_3 exchange. The branching ratio for $\tau^- \to \mu^-\phi$ is given by [121]

$$\begin{aligned}\mathcal{B}(\tau^- \to \mu^-\phi) = \frac{f_\phi^2 m_\tau^3\tau_\tau}{128\pi}\left(1-\frac{m_\phi^2}{m_\tau^2}\right)^2\Bigg\{\left(1+\frac{2m_\phi^2}{m_\tau^2}\right)\left|\left[L_{ed}^{V,LL}(m_\tau)\right]_{3222} + \left[L_{ed}^{V,LR}(m_\tau)\right]_{3222}\right|^2 \\ + \frac{8e}{m_\tau}\mathrm{Re}\left[\left[L_{e\gamma}(m_\tau)\right]_{23}(\left[L_{ed}^{V,LL}(m_\tau)\right]_{3222} + \left[L_{ed}^{V,LR}(m_\tau)\right]_{3222})\right] + \frac{16e^2}{9m_\phi^2}\left(2+\frac{m_\phi^2}{m_\tau^2}\right)\left|\left[L_{e\gamma}(m_\tau)\right]_{23}\right|^2\Bigg\},\end{aligned} \tag{60}$$

where m_ϕ and f_ϕ are the mass and the decay constant of ϕ meson, e is the electric charge, and the LEFT coefficients $[L_{ed}^{V,LL}(m_\tau)]_{3222}$, $[L_{ed}^{V,LR}(m_\tau)]_{3222}$, and $[L_{e\gamma}(m_\tau)]_{23}$ are given in Eqs. (D5), (D6), and (D9), respectively. In the current model, the branching ratio for $\tau^- \to \mu^-\phi$ is not significantly enhanced due to the smallness of the $(\bar{Y}_3^{QL})_{22}$ coupling in the tree-level contribution. As shown in Fig. 7(d), $\mathcal{B}(\tau^- \to \mu^-\phi)$ might be observed at the Belle II experiment [83]. We also consider the loop-induced LFV processes of tau lepton, $\tau^- \to \mu^-\gamma$ and $\tau^- \to \mu^-\mu^+\mu^-$. The branching ratio for $\tau^- \to \mu^-\gamma$ is given by

$$\mathcal{B}(\tau^- \to \mu^-\gamma) = \frac{m_\tau^3\tau_\tau}{4\pi}\left|[L_{e\gamma}(m_\tau)]_{23}^{\rm NP}\right|^2, \tag{61}$$

and that for $\tau^- \to \mu^-\mu^+\mu^-$ can be found, e.g., in Refs. [122,123]:

$$\mathcal{B}(\tau^- \to \mu^-\mu^+\mu^-) = \frac{m_\tau^5 \tau_\tau}{1536\pi^3}\left\{2\left|\left[L_{ee}^{V,LL}(m_\tau)\right]_{3222} + \left[L_{ee}^{V,LL}(m_\tau)\right]_{2232}\right|^2 + \left|\left[L_{ee}^{V,LR}(m_\tau)\right]_{3222}\right|^2 \right.$$
$$+ \frac{8e}{m_\tau}\mathrm{Re}\left[\left[L_{e\gamma}(m_\tau)\right]_{23}\left(2\left[L_{ee}^{V,LL}(m_\tau)\right]_{3222} + 2\left[L_{ee}^{V,LL}(m_\tau)\right]_{2232} + \left[L_{ee}^{V,LR}(m_\tau)\right]_{3222}\right)\right]$$
$$\left. + \frac{32e^2}{m_\tau^2}\left(\log\frac{m_\tau^2}{m_\mu^2} - \frac{11}{4}\right)\left|\left[L_{e\gamma}(m_\tau)\right]_{23}\right|^2\right\}. \quad (62)$$

The LEFT coefficients $[L_{ee}^{V,LL}(m_\tau)]_{2232} = [L_{ee}^{V,LL}(m_\tau)]_{3222}$, $[L_{ee}^{V,LR}(m_\tau)]_{3222}$ and $[L_{e\gamma}(m_\tau)]_{23}^{\mathrm{NP}}$, evaluated at the τ mass scale, are given in Eqs. (D7), (D8), and (D9), respectively. In the expression of $\mathcal{B}(\tau^- \to \mu^-\mu^+\mu^-)$, contributions from the RL and RR operators are neglected, since LFV occurs dominantly in the left-handed leptons in the current model. The predictions for $\mathcal{B}(\tau^- \to \mu^-\gamma)$ and $\mathcal{B}(\tau^- \to \mu^-\mu^+\mu^-)$ are shown in Figs. 7(d) and 7(e). They exhibit a strong correlation with each other, but are slightly smaller than the planned sensitivities of Belle II with 50 fb^{-1} [83].

In the current model, the muon anomalous magnetic moment (known as the muon $g-2$) is generated through the product $(Y_3^{QL})^*_{32}(Y_3^{QL})_{32}$ via the dipole coupling $[L_{e\gamma}(m_\tau)]_{22}^{\mathrm{NP}}$. We find that this contribution is too small to explain the long-standing tension between the measured value and the SM prediction of the muon $g-2$ [124,125].

The S_3 leptoquark also affects W-boson and Z-boson couplings with the SM fermions. We evaluate them with the one-loop expressions in Ref. [126], which include radiative corrections beyond the leading-logarithmic approximation. The effects on the W-boson couplings are not significant to be measured at the current and planned future experiments. We here present only the result for $\mathcal{B}(Z \to \mu^\mp\tau^\pm)$, which is calculated with the formulas given in Appendix E. Figure 7(f) shows a strong correlation between $\mathcal{B}(Z \to \mu^\mp\tau^\pm)$ and $\mathcal{B}(\tau^- \to \mu^-\gamma)$. In our scenario, the $\mathcal{B}(Z \to \mu^\mp\tau^\pm)$ can be as large as $\mathcal{O}(10^{-9})$. The present experimental bounds are given by the LEP experiment as $\mathcal{B}(Z \to \mu^\mp\tau^\pm) < 1.2 \times 10^{-5}$ [127] and the LHC experiment as $\mathcal{B}(Z \to \mu^\mp\tau^\pm) < 6.5 \times 10^{-6}$ [100]. On the other hand, the FCC-ee experiment has a sensitivity to $\mathcal{O}(10^{-9})$ [101]. In the case that $\mathcal{B}(Z \to \mu^\mp\tau^\pm)$ is enhanced enough, $\mathcal{B}(\tau^- \to \mu^-\gamma)$ is also significantly enhanced.

IV. SUMMARY

We have constructed a realistic GUT model which addresses two serious issues in the minimal SU(5) GUT: the realization of the gauge coupling unification and that of the flavor structures in the down-type-quark and the charged-lepton sectors. By introducing a 45-dimensional scalar representation Φ_{45} to the minimal SU(5) GUT, the Yukawa matrices of the down-type quarks and the charged leptons are reproduced correctly by the Georgi-Jarlskog mechanism. In addition, we have shown that the three gauge couplings can be unified through the RG running under the constraint from proton decay, if S_3, S_6, and S_8 in Φ_{45} and Σ_8 in the 24-dimensional scalar representation Σ lie much below the GUT scale. In particular, the mass of S_3, which is a scalar leptoquark, can be of the order of TeV.

The Yukawa couplings of the S_3 leptoquark at the low-energy scale is constrained by the matching condition at the GUT scale in Eq. (22). In our scenario, the S_3 leptoquark couples strongly to the SM fermions in the second and third generations, where the magnitudes of the couplings obey the hierarchy shown in Eq. (31) and Fig. 2. In particular, the coupling $(\bar{Y}_3^{QL})_{22}$ is suppressed compared with $(\bar{Y}_3^{QL})_{23}$, $(\bar{Y}_3^{QL})_{32}$, and $(\bar{Y}_3^{QL})_{33}$. The smallness of $(\bar{Y}_3^{QL})_{22}$ leads to the characteristic patterns of correlations among flavor observables.

We have investigated flavor phenomenology in this realistic GUT scenario with the S_3 leptoquark at the TeV scale. We have derived constraints on the S_3 Yukawa couplings from ΔM_s, $\mathcal{B}(B \to K^{(*)}\nu\bar{\nu})$, $R_{K^{(*)}}$, and $\mathcal{B}(B_s \to \mu^+\mu^-)$, where the results are shown in Fig. 5. We have then calculated various decays of B mesons, $\Upsilon(nS)$, tau lepton, and Z boson. In the current model, the $R(D^{(*)})$ anomaly cannot be explained by the S_3 contribution due to the strong constraints from ΔM_s and $\mathcal{B}(B \to K^{(*)}\nu\bar{\nu})$. The LFV processes $B_s \to \mu^\mp\tau^\pm$, $B^+ \to K^+\mu^-\tau^+$, and $\tau^- \to \mu^-\phi$ may be observed at Belle II with 50 ab^{-1} and LHCb with 300 fb^{-1}. It is noted that $\mathcal{B}(B^+ \to K^+\mu^+\tau^-)$ cannot reach the future sensitivity at Belle II unlike $\mathcal{B}(B^+ \to K^+\mu^-\tau^+)$. Therefore, the observation of $B^+ \to K^+\mu^-\tau^+$ together with the nonobservation of $B^+ \to K^+\mu^+\tau^-$ is a clear signal of the current model. On the other hand, it is rather hard to observe the other processes $\tau^- \to \mu^-\gamma$, $\tau^- \to \mu^-\mu^+\mu^-$, and $Z \to \mu^\mp\tau^\pm$, and much more data are needed for their observations.

In general, it is challenging to probe a GUT model, since the unification occurs at a very high-energy scale. The proton decay is a direct probe for GUT, but it has not been observed yet. We have provided a well-motivated benchmark scenario which may be able to be probed by the precise measurements of the flavor observables at the

Belle II and LHCb experiments. Besides, the S_3 leptoquark at the TeV scale can be directly searched for at the current and future hadron-collider experiments. We thus conclude that the precise flavor measurements as well as the direct searches for the S_3 leptoquark play complementary roles to the searches for proton decay in probing our GUT scenario.

ACKNOWLEDGMENTS

This work was supported in part by the Japan Society for the Promotion of Science (JSPS) KAKENHI Grants No. 17K05429 (S. M.) and No. 20H00160 (T. S.). Computations were partially carried out on the computer system (sushiki) at YITP in Kyoto University.

APPENDIX A: SCALAR POTENTIAL AND MASSES

The scalar potential $V(\Sigma, \Phi_5, \Phi_{45})$ in the SU(5)-symmetric renormalizable Lagrangian in Eq. (1) is given by

$$V(\Sigma, \Phi_5, \Phi_{45}) = V_{24} + V_5 + V_{45} + V_{24\cdot 5} + V_{24\cdot 45} + V_{5\cdot 45} + V_{24\cdot 5\cdot 45}, \tag{A1}$$

where each term is defined as

$$V_{24} = m_{24}^2 \mathrm{tr}\Sigma^2 + \chi_{24}\mathrm{tr}\Sigma^3 + \lambda_{24}^{(1)}(\mathrm{tr}\Sigma^2)^2 + \lambda_{24}^{(2)}\mathrm{tr}\Sigma^4, \tag{A2}$$

$$V_5 = m_5^2 \Phi_5^\dagger \Phi_5 + \lambda_5 (\Phi_5^\dagger \Phi_5)^2, \tag{A3}$$

$$\begin{aligned} V_{45} = {}& m_{45}^2 (\Phi_{45}^\dagger)^A_{BC}(\Phi_{45})^{BC}_A + \lambda_{45}^{(1)}[(\Phi_{45}^\dagger)^A_{BC}(\Phi_{45})^{BC}_A]^2 + \lambda_{45}^{(2)}(\Phi_{45}^\dagger)^A_{BC}(\Phi_{45})^{BC}_D(\Phi_{45}^\dagger)^D_{EF}(\Phi_{45})^{EF}_A \\ & + \lambda_{45}^{(3)}(\Phi_{45}^\dagger)^A_{BC}(\Phi_{45})^{BF}_A(\Phi_{45}^\dagger)^D_{EF}(\Phi_{45})^{EC}_D + \lambda_{45}^{(4)}(\Phi_{45}^\dagger)^A_{BC}(\Phi_{45})^{BC}_F(\Phi_{45}^\dagger)^D_{EA}(\Phi_{45})^{EF}_D \\ & + \lambda_{45}^{(5)}(\Phi_{45}^\dagger)^A_{BC}(\Phi_{45}^\dagger)^B_{AD}(\Phi_{45})^{EC}_F(\Phi_{45})^{FD}_E + \lambda_{45}^{(6)}(\Phi_{45}^\dagger)^A_{BC}(\Phi_{45}^\dagger)^B_{\mathrm{DE}}(\Phi_{45})^{CD}_F(\Phi_{45})^{EF}_A, \end{aligned} \tag{A4}$$

$$V_{24\cdot 5} = \chi_5 \Phi_5^\dagger \Sigma \Phi_5 + a^{(1)}(\mathrm{tr}\Sigma^2)\Phi_5^\dagger\Phi_5 + a^{(2)}\Phi_5^\dagger \Sigma^2 \Phi_5, \tag{A5}$$

$$\begin{aligned} V_{24\cdot 45} = {}& \chi_{45}^{(1)}(\Phi_{45}^\dagger)^A_{BC}\Sigma^D_A(\Phi_{45})^{BC}_D + \chi_{45}^{(2)}(\Phi_{45}^\dagger)^A_{BC}\Sigma^C_D(\Phi_{45})^{BD}_A + b^{(1)}(\mathrm{tr}\Sigma^2)(\Phi_{45}^\dagger)^A_{BC}(\Phi_{45})^{BC}_A \\ & + b^{(2)}(\Phi_{45}^\dagger)^A_{BC}(\Sigma^2)^D_A(\Phi_{45})^{BC}_D + b^{(3)}(\Phi_{45}^\dagger)^A_{BC}(\Sigma^2)^B_D(\Phi_{45})^{DC}_A + b^{(4)}(\Phi_{45}^\dagger)^A_{BC}\Sigma^E_A\Sigma^B_D(\Phi_{45})^{DC}_E \\ & + b^{(5)}(\Phi_{45}^\dagger)^A_{BC}\Sigma^C_E\Sigma^B_D(\Phi_{45})^{\mathrm{DE}}_A + b^{(6)}(\Phi_{45}^\dagger)^A_{BC}\Sigma^B_A\Sigma^E_D(\Phi_{45})^{DC}_E, \end{aligned} \tag{A6}$$

$$\begin{aligned} V_{5\cdot 45} = {}& c^{(1)}(\Phi_{45}^\dagger)^A_{BC}(\Phi_{45})^{BC}_A(\Phi_5^\dagger\Phi_5) + c^{(2)}(\Phi_5^\dagger)_A(\Phi_{45}^\dagger)^A_{BC}(\Phi_{45})^{BC}_D(\Phi_5)^D + c^{(3)}(\Phi_5^\dagger)_C(\Phi_{45})^{BC}_A(\Phi_{45}^\dagger)^A_{BD}(\Phi_5)^D \\ & + [c^{(4)}(\Phi_{45})^{BC}_A(\Phi_{45})^{AD}_B(\Phi_5^\dagger)_C(\Phi_5^\dagger)_D + c^{(5)}(\Phi_{45}^\dagger)^A_{BC}(\Phi_{45})^{BC}_D(\Phi_{45})^{\mathrm{DE}}_A(\Phi_5^\dagger)_E \\ & + c^{(6)}(\Phi_{45}^\dagger)^A_{BC}(\Phi_{45})^{BD}_A(\Phi_{45})^{CE}_D(\Phi_5^\dagger)_E + \mathrm{H.c.}], \end{aligned} \tag{A7}$$

$$V_{24\cdot 5\cdot 45} = \tilde{\chi}(\Phi_5^\dagger)_C\Sigma^A_B(\Phi_{45})^{BC}_A + d^{(1)}(\Phi_5^\dagger)_C(\Sigma^2)^A_B(\Phi_{45})^{BC}_A + d^{(2)}(\Phi_5^\dagger)_D\Sigma^D_C\Sigma^A_B(\Phi_{45})^{BC}_A + \mathrm{H.c.} \tag{A8}$$

The **24**-representation scalar Σ gets the VEV as

$$\langle\Sigma\rangle = \begin{pmatrix} 2v_{24} & 0 & 0 & 0 & 0 \\ 0 & 2v_{24} & 0 & 0 & 0 \\ 0 & 0 & 2v_{24} & 0 & 0 \\ 0 & 0 & 0 & -3v_{24} & 0 \\ 0 & 0 & 0 & 0 & -3v_{24} \end{pmatrix}, \tag{A9}$$

when the condition $2m_{24}^2 + 4(30\lambda_{24}^{(1)} + 7\lambda_{24}^{(2)})v_{24}^2 - 3\chi_{24}v_{24} = 0$ is satisfied [128].[4] From the potential, the squared masses of the component fields in the scalars Σ, Φ_5, and Φ_{45} can be read at the tree level as

[4]The minimization of the scalar potential for the **45** representation is studied in Refs. [129–131].

$$m_{\Sigma_1}^2=-2m_{24}^2+\frac{3}{2}\chi_{24}v_{24},\qquad m_{\Sigma_3}^2=40\lambda_{24}^{(2)}v_{24}^2-\frac{15}{2}\chi_{24}v_{24},\qquad m_{\Sigma_8}^2=10\lambda_{24}^{(2)}v_{24}^2+\frac{15}{2}\chi_{24}v_{24},$$

$$R_H^\dagger\begin{pmatrix} m_H^2 & 0\\ 0 & m_{H'}^2\end{pmatrix}R_H=\begin{pmatrix}\tilde{m}_5^2+3\tilde{a}^{(2)}v_{24}^2 & -\frac{5\sqrt{3}}{2\sqrt{2}}(\tilde{d}^{(1)}+3d^{(2)})v_{24}^2\\ -\frac{5\sqrt{3}}{2\sqrt{2}}(\tilde{d}^{(1)*}+3d^{(2)*})v_{24}^2 & \tilde{m}_{45}^2+\left(\frac{7}{4}\tilde{b}^{(2)}+\frac{19}{8}\tilde{b}^{(3)}+8b^{(4)}+\frac{17}{4}b^{(5)}+\frac{75}{8}b^{(6)}\right)v_{24}^2\end{pmatrix},$$

$$R_S^\dagger\begin{pmatrix} m_{H_C}^2 & 0\\ 0 & m_{S_1}^2\end{pmatrix}R_S=\begin{pmatrix}\tilde{m}_5^2-2\tilde{a}^{(2)}v_{24}^2 & -\frac{5}{\sqrt{2}}(\tilde{d}^{(1)}-2d^{(2)})v_{24}^2\\ -\frac{5}{\sqrt{2}}(\tilde{d}^{(1)*}-2d^{(2)*})v_{24}^2 & \tilde{m}_{45}^2+\left(\frac{1}{2}\tilde{b}^{(2)}-\frac{3}{4}\tilde{b}^{(3)}+\frac{17}{4}b^{(4)}-2b^{(5)}+\frac{25}{2}b^{(6)}\right)v_{24}^2\end{pmatrix},$$

$$m_{\tilde{S}_1}^2=\tilde{m}_{45}^2+\left(-2\tilde{b}^{(2)}+3\tilde{b}^{(3)}-\frac{9}{2}b^{(4)}+8b^{(5)}\right)v_{24}^2,\qquad m_{R_2}^2=\tilde{m}_{45}^2+\left(3\tilde{b}^{(2)}-2\tilde{b}^{(3)}-\frac{9}{2}b^{(4)}+3b^{(5)}\right)v_{24}^2,$$

$$m_{S_3}^2=\tilde{m}_{45}^2+\left(3\tilde{b}^{(2)}+\frac{1}{2}\tilde{b}^{(3)}+3b^{(4)}-7b^{(5)}\right)v_{24}^2,\qquad m_{S_6}^2=\tilde{m}_{45}^2+\left(-2\tilde{b}^{(2)}-2\tilde{b}^{(3)}+\frac{11}{2}b^{(4)}+3b^{(5)}\right)v_{24}^2,$$

$$m_{S_8}^2=\tilde{m}_{45}^2+\left(-2\tilde{b}^{(2)}+\frac{1}{2}\tilde{b}^{(3)}+\frac{1}{2}b^{(4)}-7b^{(5)}\right)v_{24}^2,\tag{A10}$$

where the following combinations of the parameters are introduced:

$$\tilde{m}_5^2=m_5^2+(30a^{(1)}+6a^{(2)})v_{24}^2,\qquad \tilde{m}_{45}^2=m_{45}^2+\left(30b^{(1)}+6b^{(2)}+6b^{(3)}-\frac{3}{2}b^{(4)}+b^{(5)}\right)v_{24}^2,$$
$$\tilde{a}^{(2)}=a^{(2)}-\frac{\chi_5}{v_{24}},\qquad \tilde{b}^{(2)}=b^{(2)}-\frac{\chi_{45}^{(1)}}{v_{24}},\qquad \tilde{b}^{(3)}=b^{(3)}-\frac{\chi_{45}^{(2)}}{v_{24}},\qquad \tilde{d}^{(1)}=d^{(1)}-\frac{\tilde{\chi}}{v_{24}},\tag{A11}$$

and the rotation matrices R_H and R_S are given as in Eq. (12):

$$R_H=\begin{pmatrix} c_H & e^{-i\delta_H}s_H\\ -e^{i\delta_H}s_H & c_H\end{pmatrix},\qquad R_S=\begin{pmatrix} c_S & e^{-i\delta_S}s_S\\ -e^{i\delta_S}s_S & c_S\end{pmatrix}.\tag{A12}$$

The masses of Σ_1, Σ_3, and Σ_8 can be freely chosen, since V_{24} in Eq. (A8) contains a sufficient number of parameters. On the other hand, the masses of the other scalars are constrained by the following relation:

$$-8(s_H^2m_H^2+c_H^2m_{H'}^2)+6(s_S^2m_{H_C}^2+c_S^2m_{S_1}^2)+6m_{\tilde{S}_1}^2-6m_{R_2}^2+9m_{S_3}^2+3m_{S_6}^2-10m_{S_8}^2=0.\tag{A13}$$

APPENDIX B: MATCHING CONDITIONS AT THE GUT SCALE

Below the GUT scale, the Yukawa interactions are given in terms of the component fields in Eqs. (6), (9), and (10) as follows:

$$\begin{aligned}-\mathcal{L}_Y={}&(Y_U)_{ij}\epsilon_{\alpha\beta}\bar{u}_{R\hat{a}i}H^\alpha q_{Lj}^{\hat{a}\beta}+(Y_D)_{ij}\bar{d}_{R\hat{a}i}H_\alpha^* q_{Lj}^{\hat{a}\alpha}+(Y_E)_{ij}\bar{e}_{Ri}H_\alpha^*\ell_{Lj}^\alpha\\ &+(Y'_U)_{ij}\epsilon_{\alpha\beta}\bar{u}_{R\hat{a}i}H'^\alpha q_{Lj}^{\hat{a}\beta}+(Y'_D)_{ij}\bar{d}_{R\hat{a}i}H_\alpha'^* q_{Lj}^{\hat{a}\alpha}+(Y'_E)_{ij}\bar{e}_{Ri}H_\alpha'^*\ell_{Lj}^\alpha\\ &+(Y_C^{QL})_{ij}\epsilon_{\alpha\beta}\bar{q}_{Li}^{c\hat{a}\alpha}H_{C\hat{a}}\ell_{Lj}^\beta+(Y_C^{UE})_{ij}\bar{u}_{R\hat{a}i}H_C^{*\hat{a}}e_{Rj}^c+(Y_C^{DU})_{ij}\epsilon^{\hat{a}\hat{b}\hat{c}}\bar{d}_{R\hat{a}i}H_{C\hat{b}}u_{R\hat{c}j}^c+\frac{(Y_C^{QQ})_{ij}}{2}\epsilon_{\hat{a}\hat{b}\hat{c}}\epsilon_{\alpha\beta}\bar{q}_{Li}^{c\hat{a}\alpha}H_C^{*\hat{b}}q_{Lj}^{\hat{c}\beta}\\ &+(Y_1^{QL})_{ij}\epsilon_{\alpha\beta}\bar{q}_{Li}^{c\hat{a}\alpha}S_{1\hat{a}}\ell_{Lj}^\beta+(Y_1^{UE})_{ij}\bar{u}_{R\hat{a}i}S_1^{*\hat{a}}e_{Rj}^c+(Y_1^{DU})_{ij}\epsilon^{\hat{a}\hat{b}\hat{c}}\bar{d}_{R\hat{a}i}S_{1\hat{b}}u_{R\hat{c}j}^c+\frac{(Y_1^{QQ})_{ij}}{2}\epsilon_{\hat{a}\hat{b}\hat{c}}\epsilon_{\alpha\beta}\bar{q}_{Li}^{c\hat{a}\alpha}S_1^{*\hat{b}}q_{Lj}^{\hat{c}\beta}\\ &+(\tilde{Y}_1^{ED})_{ij}\bar{e}_{Ri}\tilde{S}_1^{*\hat{a}}d_{R\hat{a}j}^c+\frac{(\tilde{Y}_1^{UU})_{ij}}{2}\epsilon^{\hat{a}\hat{b}\hat{c}}\bar{u}_{R\hat{a}i}\tilde{S}_{1\hat{b}}u_{R\hat{c}j}^c+(Y_2^{UL})_{ij}\epsilon_{\alpha\beta}\bar{u}_{R\hat{a}i}R_2^{\hat{a}\alpha}\ell_{Lj}^\beta+(Y_2^{EQ})_{ij}\bar{e}_{Ri}R_{2\hat{a}\alpha}^* q_{Lj}^{\hat{a}\alpha}\end{aligned}$$

$$
\begin{aligned}
&+ (Y_3^{QL})_{ij}\epsilon_{\alpha\beta}\bar{q}_{Li}^{\hat{c}\hat{a}\gamma}(\sigma_a)^{\alpha}{}_{\gamma}S_{3\hat{a}}^{a}\ell_{Lj}^{\beta} + \frac{(Y_3^{QQ})_{ij}}{2}\epsilon_{\hat{a}\hat{b}\hat{c}}\epsilon_{\alpha\beta}\bar{q}_{Li}^{\hat{c}\hat{a}\alpha}(\sigma^a)^{\beta}{}_{\gamma}S_3^{*a\hat{b}}q_{Lj}^{\hat{c}\gamma} \\
&+ (Y_6^{DU})_{ij}\bar{d}_{R\hat{a}i}(\eta^A)^{\hat{a}\hat{b}}S_6^A u_{R\hat{b}j}^c + \frac{(Y_6^{QQ})_{ij}}{2}\epsilon_{\alpha\beta}\bar{q}_{Li}^{\hat{c}\hat{a}\alpha}(\eta^A)_{\hat{a}\hat{b}}S_6^{A*}q_{Lj}^{\hat{b}\beta} \\
&+ (Y_8^{UQ})_{ij}\epsilon_{\alpha\beta}\bar{u}_{R\hat{a}i}(\lambda^A)^{\hat{a}}{}_{\hat{b}}S_8^{A\alpha}q_{Lj}^{\hat{b}\beta} + (Y_8^{DQ})_{ij}\bar{d}_{R\hat{a}i}(\lambda^A)^{\hat{a}}{}_{\hat{b}}S_{8\alpha}^{A*}q_{Lj}^{\hat{b}\alpha} + \text{H.c.},
\end{aligned} \tag{B1}
$$

where Y_C^{QQ} and Y_1^{QQ} are symmetric matrices in the flavor space, while $\tilde{Y}_1^{UU}$, Y_3^{QQ}, and Y_6^{QQ} are antisymmetric matrices:

$$
(Y_C^{QQ})^T = Y_C^{QQ}, \qquad (Y_1^{QQ})^T = Y_1^{QQ}, \qquad (\tilde{Y}_1^{UU})^T = -\tilde{Y}_1^{UU}, \qquad (Y_3^{QQ})^T = -Y_3^{QQ}, \qquad (Y_6^{QQ})^T = -Y_6^{QQ}. \tag{B2}
$$

The Yukawa couplings in Eq. (B1) are matched onto those in Eq. (3) at the tree level as

$$
\begin{aligned}
&Y_U = -\frac{1}{2}V_{QU}^T\left(c_H Y_5^U + \sqrt{\frac{2}{3}}e^{i\delta_H}s_H Y_{45}^U\right)^T, && Y'_U = \frac{1}{2}V_{QU}^T\left(e^{-i\delta_H}s_H Y_5^U - \sqrt{\frac{2}{3}}c_H Y_{45}^U\right)^T, \\
&Y_D = -\frac{1}{\sqrt{2}}\left(c_H Y_5^D - \frac{1}{2\sqrt{6}}e^{-i\delta_H}s_H Y_{45}^D\right)^T, && Y'_D = \frac{1}{\sqrt{2}}\left(e^{i\delta_H}s_H Y_5^D + \frac{1}{2\sqrt{6}}c_H Y_{45}^D\right)^T, \\
&Y_E = -\frac{1}{\sqrt{2}}V_{QE}^T\left(c_H Y_5^D + \frac{\sqrt{3}}{2\sqrt{2}}e^{-i\delta_H}s_H Y_{45}^D\right)V_{DL}, && Y'_E = \frac{1}{\sqrt{2}}V_{QE}^T\left(e^{i\delta_H}s_H Y_5^D - \frac{\sqrt{3}}{2\sqrt{2}}c_H Y_{45}^D\right)V_{DL}, \\
&Y_C^{QL} = \frac{1}{\sqrt{2}}\left(c_S Y_5^D + \frac{1}{2\sqrt{2}}e^{i\delta_S}s_S Y_{45}^D\right)V_{DL}, && Y_1^{QL} = \frac{1}{\sqrt{2}}\left(-e^{-i\delta_S}s_S Y_5^D + \frac{1}{2\sqrt{2}}c_S Y_{45}^D\right)V_{DL}, \\
&Y_C^{UE} = \frac{1}{2}V_{QU}^T\left(c_S Y_5^U - \sqrt{2}e^{-i\delta_S}s_S Y_{45}^U\right)V_{QE}, && Y_1^{UE} = -\frac{1}{2}V_{QU}^T\left(e^{i\delta_S}s_S Y_5^U + \sqrt{2}c_S Y_{45}^U\right)V_{QE}, \\
&Y_C^{DU} = \frac{1}{\sqrt{2}}\left(-c_S Y_5^D + \frac{1}{2\sqrt{2}}e^{i\delta_S}s_S Y_{45}^D\right)^T V_{QU}, && Y_1^{DU} = \frac{1}{\sqrt{2}}\left(e^{-i\delta_S}s_S Y_5^D + \frac{1}{2\sqrt{2}}c_S Y_{45}^D\right)^T V_{QU}, \\
&Y_C^{QQ} = \frac{1}{2}c_S Y_5^U, \quad Y_1^{QQ} = -\frac{1}{2}e^{i\delta_S}s_S Y_5^U, && \tilde{Y}_1^{UU} = \frac{1}{\sqrt{2}}V_{QU}^T Y_{45}^U V_{QU}, \quad \tilde{Y}_1^{ED} = \frac{1}{2}V_{QE}^T Y_{45}^D, \\
&Y_2^{EQ} = \frac{1}{\sqrt{2}}V_{QE}^T Y_{45}^U, \quad Y_2^{UL} = \frac{1}{2}V_{QU}^T Y_{45}^D V_{DL}, && Y_3^{QQ} = \frac{1}{2}Y_{45}^U, \quad Y_3^{QL} = -\frac{1}{2\sqrt{2}}Y_{45}^D V_{DL}, \\
&Y_6^{QQ} = -\frac{1}{\sqrt{2}}Y_{45}^U, \quad Y_6^{DU} = \frac{1}{2}(Y_{45}^D)^T V_{QU}, && Y_8^{UQ} = -\frac{1}{2}V_{QU}^T Y_{45}^U, \quad Y_8^{DQ} = \frac{1}{2\sqrt{2}}(Y_{45}^D)^T.
\end{aligned} \tag{B3}
$$

APPENDIX C: RENORMALIZATION GROUP EQUATIONS

The scale dependence of the gauge couplings is governed by the RGEs,

$$
\frac{dg_i}{d\log\mu} = \frac{\beta_{g_i}}{(4\pi)^2}, \tag{C1}
$$

where $g_i = g_s$, g and g', and β_{g_i} denotes the corresponding beta function. The one-loop contributions to the beta functions are given by

$$
\beta_{g_i} = \left[B_{g_i}^{\text{SM}} + \sum_{\phi} B_{g_i}^{\phi}\theta(m_\phi - \mu)\right]g_i^3, \tag{C2}
$$

where $\phi = H'$, H_C, S_1, $\tilde{S}_1$, R_2, S_3, S_6, S_8, Σ_1, Σ_3, and Σ_8, and the coefficients $B_{g_i}^{\text{SM}}$ and $B_{g_i}^{\phi}$ are listed in Table IV.

The RGEs of the Yukawa couplings $Y_{\bar{\psi}\psi'}^{\phi}$ associated with the interaction of the form $[Y_{\bar{\psi}\psi'}^{\phi}]_{jk}\bar{\psi}_j\phi\psi'_k$ are given by

$$
\frac{d}{d\log\mu}Y_{\bar{\psi}\psi'}^{\phi} = \frac{1}{(4\pi)^2}\beta_{Y_{\bar{\psi}\psi'}^{\phi}}, \tag{C3}
$$

where the one-loop beta functions can generally be written as [132–135]

$$
\begin{aligned}
\beta_{Y_{\bar{\psi}\psi'}^{\phi}} &= -3\sum_i g_i^2[C_2^i(\psi)Y_{\bar{\psi}\psi'}^{\phi} + Y_{\bar{\psi}\psi'}^{\phi}C_2^i(\psi')] \\
&\quad + \frac{1}{2}[Y_2(\psi)Y_{\bar{\psi}\psi'}^{\phi} + Y_{\bar{\psi}\psi'}^{\phi}Y_2(\psi')] \\
&\quad + Y_{\bar{\psi}\psi'}^{\phi}\Theta(\phi) + 2\Gamma_{Y_{\bar{\psi}\psi'}^{\phi}}.
\end{aligned} \tag{C4}
$$

TABLE IV. $B^{\rm SM}_{g_i}$ and $B^{\phi}_{g_i}$ for the RGEs of the gauge couplings.

g_i	$B^{\rm SM}_{g_i}$	$B^{H'}_{g_i}$	$B^{H_C}_{g_i}$	$B^{S_1}_{g_i}$	$B^{\tilde{S}_1}_{g_i}$	$B^{R_2}_{g_i}$	$B^{S_3}_{g_i}$	$B^{S_6}_{g_i}$	$B^{S_8}_{g_i}$	$B^{\Sigma_1}_{g_i}$	$B^{\Sigma_3}_{g_i}$	$B^{\Sigma_8}_{g_i}$
g_s	−7	0	1/6	1/6	1/6	1/3	1/2	5/6	2	0	0	1/2
g	−19/6	1/6	0	0	0	1/2	2	0	4/3	0	1/3	0
g'	41/6	1/6	1/9	1/9	16/9	49/18	1/3	2/9	4/3	0	0	0

Below we list explicit formulas for the Yukawa couplings defined in Eq. (B1)[5]: $Y^{\phi}_{\bar{\psi}\psi'} = Y_U, Y_D, Y_E, Y'_U, Y'_D, Y'_E, Y^{QL}_C, Y^{UE}_C, Y^{DU}_C, Y^{QQ}_C, Y^{QL}_1, Y^{UE}_1, Y^{DU}_1, Y^{QQ}_1, \tilde{Y}^{ED}_1, \tilde{Y}^{UU}_1, Y^{UL}_2, Y^{EQ}_2, Y^{QL}_3, Y^{QQ}_3, Y^{DU}_6, Y^{QQ}_6, Y^{UQ}_8$, and Y^{DQ}_8. In the beta functions, the coupling $Y^{\phi}_{\bar{\psi}\psi'}$ should be understood as $Y^{\phi}_{\bar{\psi}\psi'}\theta(m_\phi - \mu)$ by considering the decoupling of heavy particles, and for $\phi = H, H', H_C$ and S_1, the term $Y^{\phi}_{\bar{\psi}\psi'}\Theta(\phi)$ is replaced as

$$Y^{\phi}_{\bar{\psi}\psi'}\Theta(\phi) \to \begin{cases} Y^{H}_{\bar{\psi}\psi'}\Theta(H) + Y^{H'}_{\bar{\psi}\psi'}\Theta(H'^{*}H) & \text{for } \phi = H, \\ Y^{H'}_{\bar{\psi}\psi'}\Theta(H') + Y^{H}_{\bar{\psi}\psi'}\Theta(H^{*}H') & \text{for } \phi = H', \\ Y^{H_C}_{\bar{\psi}\psi'}\Theta(H_C) + Y^{S_1}_{\bar{\psi}\psi'}\Theta(S_1^{*}H_C) & \text{for } \phi = H_C, \\ Y^{S_1}_{\bar{\psi}\psi'}\Theta(S_1) + Y^{H_C}_{\bar{\psi}\psi'}\Theta(H_C^{*}S_1) & \text{for } \phi = S_1. \end{cases} \tag{C5}$$

(1) Gauge-boson-loop contributions:

$$\sum_i g_i^2 C_2^i(q_L) = \frac{4}{3}g_s^2 + \frac{3}{4}g^2 + \frac{1}{36}g'^2, \qquad \sum_i g_i^2 C_2^i(u_R) = \frac{4}{3}g_s^2 + \frac{4}{9}g'^2, \qquad \sum_i g_i^2 C_2^i(d_R) = \frac{4}{3}g_s^2 + \frac{1}{9}g'^2,$$
$$\sum_i g_i^2 C_2^i(\ell_L) = \frac{3}{4}g^2 + \frac{1}{4}g'^2, \qquad \sum_i g_i^2 C_2^i(e_R) = g'^2, \tag{C6}$$

where $C_2^i(\psi^c) = C_2^i(\psi)$.

(2) Self-energy contributions to the fermions:

$$\begin{aligned} Y_2(q_L) &= Y_U^\dagger Y_U + Y_D^\dagger Y_D + Y'^\dagger_U Y'_U + Y'^\dagger_D Y'_D + Y^{QL*}_C (Y^{QL}_C)^T + 2Y^{QQ\dagger}_C Y^{QQ}_C + Y^{QL*}_1 (Y^{QL}_1)^T + 2Y^{QQ\dagger}_1 Y^{QQ}_1 \\ &\quad + Y^{EQ\dagger}_2 Y^{EQ}_2 + 6Y^{QQ\dagger}_3 Y^{QQ}_3 + 3Y^{QL*}_3 (Y^{QL}_3)^T + 2Y^{QQ\dagger}_6 Y^{QQ}_6 + \frac{16}{3}Y^{UQ\dagger}_8 Y^{UQ}_8 + \frac{16}{3}Y^{DQ\dagger}_8 Y^{DQ}_8, \\ Y_2(u_R) &= 2Y_U Y_U^\dagger + 2Y'_U Y'^\dagger_U + Y^{UE}_C Y^{UE\dagger}_C + 2(Y^{DU}_C)^T Y^{DU*}_C + Y^{UE}_1 Y^{UE\dagger}_1 + 2(Y^{DU}_1)^T Y^{DU*}_1 + 2\tilde{Y}^{UU}_1 \tilde{Y}^{UU\dagger}_1 \\ &\quad + 2Y^{UL}_2 Y^{UL\dagger}_2 + 2(Y^{DU}_6)^T Y^{DU*}_6 + \frac{32}{3}Y^{UQ}_8 Y^{UQ\dagger}_8, \\ Y_2(d_R) &= 2Y_D Y_D^\dagger + 2Y'_D Y'^\dagger_D + 2Y^{DU}_C Y^{DU\dagger}_C + 2Y^{DU}_1 Y^{DU\dagger}_1 + (\tilde{Y}^{ED}_1)^T \tilde{Y}^{ED*}_1 + 2Y^{DU}_6 Y^{DU\dagger}_6 + \frac{32}{3}Y^{DQ}_8 Y^{DQ\dagger}_8, \\ Y_2(\ell_L) &= Y_E^\dagger Y_E + Y'^\dagger_E Y'_E + 3Y^{QL\dagger}_C Y^{QL}_C + 3Y^{QL\dagger}_1 Y^{QL}_1 + 3Y^{UL\dagger}_2 Y^{UL}_2 + 9Y^{QL\dagger}_3 Y^{QL}_3, \\ Y_2(e_R) &= 2Y_E Y_E^\dagger + 2Y'_E Y'^\dagger_E + 3(Y^{UE}_C)^T Y^{UE*}_C + 3(Y^{UE}_1)^T Y^{UE*}_1 + 3\tilde{Y}^{ED}_1 \tilde{Y}^{ED\dagger}_1 + 6Y^{EQ}_2 Y^{EQ\dagger}_2, \end{aligned} \tag{C7}$$

where $Y_2(\psi^c) = [Y_2(\psi)]^T$.

[5]The RGEs for the SM, S_1, and S_3 Yukawa couplings were recently studied in Refs. [136,137].

(3) Self-energy contributions to the scalars:

$$\begin{aligned}
\Theta(H) &= \mathrm{tr}(3Y_U^\dagger Y_U + 3Y_D^\dagger Y_D + Y_E^\dagger Y_E), \qquad \Theta(H') = \mathrm{tr}(3Y_U'^\dagger Y_U' + 3Y_D'^\dagger Y_D' + Y_E'^\dagger Y_E'),\\
\Theta(H_C) &= \mathrm{tr}(2Y_C^{QL\dagger} Y_C^{QL} + Y_C^{UE\dagger} Y_C^{UE} + 2Y_C^{DU\dagger} Y_C^{DU} + 2Y_C^{QQ\dagger} Y_C^{QQ}),\\
\Theta(S_1) &= \mathrm{tr}(2Y_1^{QL\dagger} Y_1^{QL} + Y_1^{UE\dagger} Y_1^{UE} + 2Y_1^{DU\dagger} Y_1^{DU} + 2Y_1^{QQ\dagger} Y_1^{QQ}),\\
\Theta(\tilde{S}_1) &= \mathrm{tr}(\tilde{Y}_1^{ED\dagger} \tilde{Y}_1^{ED} + \tilde{Y}_1^{UU\dagger} \tilde{Y}_1^{UU}), \qquad \Theta(R_2) = \mathrm{tr}(Y_2^{UL\dagger} Y_2^{UL} + Y_2^{EQ\dagger} Y_2^{EQ}),\\
\Theta(S_3) &= \mathrm{tr}(2Y_3^{QL\dagger} Y_3^{QL} + 2Y_3^{QQ\dagger} Y_3^{QQ}), \qquad \Theta(S_6) = \mathrm{tr}(Y_6^{DU\dagger} Y_6^{DU} + Y_6^{QQ\dagger} Y_6^{QQ}),\\
\Theta(S_8) &= \mathrm{tr}(2Y_8^{DQ\dagger} Y_8^{DQ} + 2Y_8^{UQ\dagger} Y_8^{UQ}), \qquad \Theta(H^* H') = \mathrm{tr}(3Y_U^\dagger Y_U' + 3Y_D Y_D'^\dagger + Y_E Y_E'^\dagger),\\
\Theta(S_1^* H_C) &= \mathrm{tr}(2Y_1^{QL\dagger} Y_C^{QL} + Y_1^{UE} Y_C^{UE\dagger} + 2Y_1^{DU\dagger} Y_C^{DU} + 2Y_1^{QQ} Y_C^{QQ\dagger}),
\end{aligned} \tag{C8}$$

where $\Theta(\phi^*) = \Theta(\phi)$, $\Theta(H'^* H) = [\Theta(H^* H')]^*$, and $\Theta(H_C^* S_1) = [\Theta(S_1^* H_C)]^*$.

(4) Vertex corrections:

$$\begin{aligned}
\Gamma_{Y_U^{(\prime)}} &= -Y_U Y_D^{(\prime)\dagger} Y_D - Y_U' Y_D^{(\prime)\dagger} Y_D' - Y_C^{UE} Y_E^{(\prime)*} (Y_C^{QL})^T + 2(Y_C^{DU})^T Y_D^{(\prime)*} Y_C^{QQ} - Y_1^{UE} Y_E^{(\prime)*} (Y_1^{QL})^T\\
&\quad + 2(Y_1^{DU})^T Y_D^{(\prime)*} Y_1^{QQ} - Y_2^{UL} Y_E^{(\prime)\dagger} Y_2^{EQ} + 2(Y_6^{DU})^T Y_D^{(\prime)*} Y_6^{QQ} - \frac{16}{3} Y_8^{UQ} Y_D^{(\prime)\dagger} Y_8^{DQ},\\
\Gamma_{Y_D^{(\prime)}} &= -Y_D Y_U^{(\prime)\dagger} Y_U - Y_D' Y_U^{(\prime)\dagger} Y_U' + 2Y_C^{DU} Y_U^{(\prime)*} Y_C^{QQ} + 2Y_1^{DU} Y_U^{(\prime)*} Y_1^{QQ} - 2Y_6^{DU} Y_U^{(\prime)*} Y_6^{QQ} - \frac{16}{3} Y_8^{DQ} Y_U^{(\prime)\dagger} Y_8^{UQ},\\
\Gamma_{Y_E^{(\prime)}} &= -3(Y_C^{UE})^T Y_U^{(\prime)*} Y_C^{QL} - 3(Y_1^{UE})^T Y_U^{(\prime)*} Y_1^{QL} - 3Y_2^{EQ} Y_U^{(\prime)\dagger} Y_2^{UL},\\
\Gamma_{Y_i^{QL}} &= -Y_U^T Y_i^{UE*} Y_E - Y_U'^T Y_i^{UE*} Y_E' - 2Y_C^{QQ} Y_i^{QQ\dagger} Y_C^{QL} - 2Y_1^{QQ} Y_i^{QQ\dagger} Y_1^{QL} + (Y_2^{EQ})^T Y_i^{UE\dagger} Y_2^{UL}\\
&\quad + 6Y_3^{QQ} Y_i^{QQ\dagger} Y_3^{QL} (i = C, 1),\\
\Gamma_{Y_i^{UE}} &= -2Y_U Y_i^{QL*} Y_E^T - 2Y_U' Y_i^{QL*} Y_E'^T - 2(Y_C^{DU})^T Y_i^{DU*} Y_C^{UE} - 2(Y_1^{DU})^T Y_i^{DU*} Y_1^{UE} - 2\tilde{Y}_1^{UU} Y_i^{DU\dagger} (\tilde{Y}_1^{ED})^T\\
&\quad + 2Y_2^{UL} Y_i^{QL\dagger} (Y_2^{EQ})^T (i = C, 1),\\
\Gamma_{Y_i^{DU}} &= 2Y_D Y_i^{QQ\dagger} Y_U^T + 2Y_D' Y_i^{QQ\dagger} Y_U'^T - Y_C^{DU} Y_i^{UE*} (Y_C^{UE})^T - Y_1^{DU} Y_i^{UE*} (Y_1^{UE})^T - (\tilde{Y}_1^{ED})^T Y_i^{UE\dagger} \tilde{Y}_1^{UU}\\
&\quad - \frac{16}{3} Y_8^{DQ} Y_i^{QQ\dagger} (Y_8^{UQ})^T (i = C, 1),\\
\Gamma_{Y_i^{QQ}} &= Y_D^T Y_i^{DU*} Y_U + Y_U^T Y_i^{DU\dagger} Y_D + Y_D'^T Y_i^{DU*} Y_U' + Y_U'^T Y_i^{DU\dagger} Y_D' - Y_C^{QL} Y_i^{QL\dagger} Y_C^{QQ} - Y_C^{QQ} Y_i^{QL*} (Y_C^{QL})^T\\
&\quad - Y_1^{QL} Y_i^{QL\dagger} Y_1^{QQ} - Y_1^{QQ} Y_i^{QL*} (Y_1^{QL})^T - 3Y_3^{QQ} Y_i^{QL*} (Y_3^{QL})^T + 3Y_3^{QL} Y_i^{QL\dagger} Y_3^{QQ}\\
&\quad - \frac{8}{3} (Y_8^{UQ})^T Y_i^{DU\dagger} Y_8^{DQ} - \frac{8}{3} (Y_8^{DQ})^T Y_i^{DU*} Y_8^{UQ} (i = C, 1),\\
\Gamma_{\tilde{Y}_1^{ED}} &= 2(Y_C^{UE})^T \tilde{Y}_1^{UU\dagger} (Y_C^{DU})^T + 2(Y_1^{UE})^T \tilde{Y}_1^{UU\dagger} (Y_1^{DU})^T,\\
\Gamma_{\tilde{Y}_1^{UU}} &= -Y_C^{UE} \tilde{Y}_1^{ED*} Y_C^{DU} + (Y_C^{DU})^T \tilde{Y}_1^{ED\dagger} (Y_C^{UE})^T - Y_1^{UE} \tilde{Y}_1^{ED*} Y_1^{DU} + (Y_1^{DU})^T \tilde{Y}_1^{ED\dagger} (Y_1^{UE})^T,\\
\Gamma_{Y_2^{UL}} &= -Y_U Y_2^{EQ\dagger} Y_E - Y_U' Y_2^{EQ\dagger} Y_E' + Y_C^{UE} Y_2^{EQ*} Y_C^{QL} + Y_1^{UE} Y_2^{EQ*} Y_1^{QL},\\
\Gamma_{Y_2^{EQ}} &= -Y_E Y_2^{UL\dagger} Y_U - Y_E' Y_2^{UL\dagger} Y_U' + (Y_C^{UE})^T Y_2^{UL*} (Y_C^{QL})^T + (Y_1^{UE})^T Y_2^{UL*} (Y_1^{QL})^T,\\
\Gamma_{Y_3^{QL}} &= 2Y_C^{QQ} Y_3^{QQ\dagger} Y_C^{QL} + 2Y_1^{QQ} Y_3^{QQ\dagger} Y_1^{QL} + 2Y_3^{QQ} Y_3^{QQ\dagger} Y_3^{QL},\\
\Gamma_{Y_3^{QQ}} &= -Y_C^{QQ} Y_3^{QL*} (Y_C^{QL})^T + Y_C^{QL} Y_3^{QL\dagger} Y_C^{QQ} - Y_1^{QQ} Y_3^{QL*} (Y_1^{QL})^T + Y_1^{QL} Y_3^{QL\dagger} Y_1^{QQ} + Y_3^{QQ} Y_3^{QL*} (Y_3^{QL})^T\\
&\quad + Y_3^{QL} Y_3^{QL\dagger} Y_3^{QQ},\\
\Gamma_{Y_6^{DU}} &= -2Y_D Y_6^{QQ\dagger} Y_U^T - 2Y_D' Y_6^{QQ\dagger} Y_U'^T - \frac{8}{3} Y_8^{DQ} Y_6^{QQ\dagger} (Y_8^{UQ})^T,
\end{aligned}$$

$$\Gamma_{Y_6^{QQ}} = -Y_U^T Y_6^{DU\dagger} Y_D + Y_D^T Y_6^{DU*} Y_U - Y_U'^T Y_6^{DU\dagger} Y_D' + Y_D'^T Y_6^{DU*} Y_U' - \frac{4}{3}(Y_8^{UQ})^T Y_6^{DU\dagger} Y_8^{DQ} + \frac{4}{3}(Y_8^{DQ})^T Y_6^{DU*} Y_8^{UQ},$$

$$\Gamma_{Y_8^{UQ}} = -Y_U Y_8^{DQ\dagger} Y_D - Y_U' Y_8^{DQ\dagger} Y_D' - (Y_C^{DU})^T Y_8^{DQ*} Y_C^{QQ} - (Y_1^{DU})^T Y_8^{DQ*} Y_1^{QQ} + \frac{1}{2}(Y_6^{DU})^T Y_8^{DQ*} Y_6^{QQ} + \frac{2}{3} Y_8^{UQ} Y_8^{DQ\dagger} Y_8^{DQ},$$

$$\Gamma_{Y_8^{DQ}} = -Y_D Y_8^{UQ\dagger} Y_U - Y_D' Y_8^{UQ\dagger} Y_U' - Y_C^{DU} Y_8^{UQ*} Y_C^{QQ} - Y_1^{DU} Y_8^{UQ*} Y_1^{QQ} - \frac{1}{2} Y_6^{DU} Y_8^{UQ*} Y_6^{QQ} + \frac{2}{3} Y_8^{DQ} Y_8^{UQ\dagger} Y_8^{UQ}. \tag{C9}$$

Notice that the coupling Y_3^{QQ} is shown to be vanishing in the whole range of the renormalization scale below the GUT scale if $Y_3^{QQ} = 0$ and H_C, S_1, and $\tilde{S}_1$ decouple at the GUT scale. In fact, the Yukawa interaction Lagrangian in Eq. (B1) becomes invariant under $U(1)_B$ and $U(1)_L$ separately if the terms with H_C, S_1, and $\tilde{S}_1$ are removed and if Y_3^{QQ} is set to vanish. The latter condition is satisfied if $Y_{45}^U = 0$ at the GUT scale in the tree-level approximation. The appropriate assignment of the baryon and lepton numbers in the above case is listed in Table V.

APPENDIX D: LEFT LAGRANGIAN

The LEFT Lagrangian is given by

$$\mathcal{L}_{\rm LEFT} = \mathcal{L}_{\rm QCD+QED} + \sum_i L_i \mathcal{Q}_i, \tag{D1}$$

where $\mathcal{L}_{\rm QCD+QED}$ is the renormalizable QCD and QED Lagrangian with the SM fermions except for top quark. The LEFT operators $\mathcal{Q}_i$ up to dimension six are classified in Ref. [65]. The operators relevant to the current study are

$$\begin{aligned}
[\mathcal{Q}_{\nu d}^{V,LL}]_{ijkl} &= (\bar{\hat{\nu}}_{Li}\gamma^\mu \hat{\nu}_{Lj})(\bar{\hat{d}}_{Lk}\gamma_\mu \hat{d}_{Ll}), & [\mathcal{Q}_{ed}^{V,LL}]_{ijkl} &= (\bar{\hat{e}}_{Li}\gamma^\mu \hat{e}_{Lj})(\bar{\hat{d}}_{Lk}\gamma_\mu \hat{d}_{Ll}), \\
[\mathcal{Q}_{ee}^{V,LL}]_{ijkl} &= (\bar{\hat{e}}_{Li}\gamma^\mu \hat{e}_{Lj})(\bar{\hat{e}}_{Lk}\gamma_\mu \hat{e}_{Ll}), & [\mathcal{Q}_{ee}^{V,LR}]_{ijkl} &= (\bar{\hat{e}}_{Li}\gamma^\mu \hat{e}_{Lj})(\bar{\hat{e}}_{Rk}\gamma_\mu \hat{e}_{Rl}), \\
[\mathcal{Q}_{dd}^{V,LL}]_{ijkl} &= (\bar{\hat{d}}_{Li}\gamma^\mu \hat{d}_{Lj})(\bar{\hat{d}}_{Lk}\gamma_\mu \hat{d}_{Ll}), & [\mathcal{Q}_{e\gamma}]_{ij} &= (\bar{\hat{e}}_{Li}\sigma^{\mu\nu} \hat{e}_{Rj})F_{\mu\nu}, \\
[\mathcal{Q}_{ed}^{V,LR}]_{ijkl} &= (\bar{\hat{e}}_{Li}\gamma^\mu \hat{e}_{Lj})(\bar{\hat{d}}_{Rk}\gamma_\mu \hat{d}_{Rl}), & [\mathcal{Q}_{de}^{V,LR}]_{ijkl} &= (\bar{\hat{d}}_{Li}\gamma^\mu \hat{d}_{Lj})(\bar{\hat{e}}_{Rk}\gamma_\mu \hat{e}_{Rl}), \\
[\mathcal{Q}_{\nu edu}^{V,LL}]_{ijkl} &= (\bar{\hat{\nu}}_{Li}\gamma^\mu \hat{e}_{Lj})(\bar{\hat{d}}_{Lk}\gamma_\mu \hat{u}_{Ll}),
\end{aligned} \tag{D2}$$

where there also exist the Hermitian conjugates of the non-self-conjugate operators.

The Wilson coefficients for these operators are calculated as follows.

(1) The S_3 field is integrated out at the S_3 mass scale, and the model is matched onto the SMEFT at the one-loop level. The one-loop matching formulas from a model with the S_1 and S_3 leptoquarks to the SMEFT are listed in Refs. [58–60].

(2) The RG running effects of the SMEFT operators are taken into account. The anomalous dimensions for the dimension-six operators in the SMEFT are listed in Refs. [61–63].

(3) The SMEFT is matched onto the LEFT at the weak scale. The one-loop matching formulas are listed in Refs. [65–67].

(4) The RG effects in the LEFT are taken into account. The corresponding anomalous dimensions are given in Refs. [68,69].

The coefficients in the LEFT Lagrangian at the relevant scale for the process under consideration are given in the leading-logarithmic approximation by

TABLE V. Assignment of the baryon and lepton numbers to the scalars, where the Yukawa interactions in Eq. (B1) are invariant under $U(1)_B$ and $U(1)_L$ separately if H_C, S_1, and $\tilde{S}_1$ decouple and Y_3^{QQ} is set to vanish at the GUT scale.

	R_2^*	S_3^*	S_6^*	S_8
$3B$	−1	1	−2	0
L	1	1	0	0

$$
\begin{aligned}
[L_{\nu d}^{V,LL}]^{\rm NP}_{ij23} = & \frac{(\bar{Y}_3^{QL})^*_{2i}(\bar{Y}_3^{QL})_{3j}}{2m_{S_3}^2}\left\{1+\frac{g^2(1+2c_W^2)}{32\pi^2c_W^2}\left[\log\left(\frac{m_{S_3}^2}{m_Z^2}\right)+\frac{11}{6}\right]-\frac{3g^2}{16\pi^2}\left[\log\left(\frac{m_{S_3}^2}{m_W^2}\right)+\frac{11}{6}\right]\right\} \\
& +\frac{y_t^2}{64\pi^2}\left\{4V_{ts}^*V_{tb}\frac{(Y_3^{QL})^*_{3i}(Y_3^{QL})_{3j}}{m_{S_3}^2}+\frac{1}{2}\left[V_{ts}^*\frac{(Y_3^{QL})^*_{3i}(\bar{Y}_3^{QL})_{3j}}{m_{S_3}^2}+V_{tb}\frac{(\bar{Y}_3^{QL})^*_{2i}(Y_3^{QL})_{3j}}{m_{S_3}^2}\right]I_{\nu d}(x_t)\right\} \\
& -\frac{3(N_c+1)}{16}\left[\frac{(\bar{Y}_3^{QL\dagger}\bar{Y}_3^{QL}\bar{Y}_3^{QL\dagger})_{i2}(\bar{Y}_3^{QL})_{3j}}{(4\pi)^2m_{S_3}^2}+\frac{(\bar{Y}_3^{QL})^*_{2i}(\bar{Y}_3^{QL}\bar{Y}_3^{QL\dagger}\bar{Y}_3^{QL})_{3j}}{(4\pi)^2m_{S_3}^2}\right] \\
& -\frac{1}{4}\frac{(\bar{Y}_3^{QL\dagger}\bar{Y}_3^{QL})_{ij}(\bar{Y}_3^{QL}\bar{Y}_3^{QL\dagger})_{32}}{(4\pi)^2m_{S_3}^2},
\end{aligned}
\tag{D3}
$$

$$
[L_{de}^{V,LR}(m_b)]^{\rm NP}_{23ij} = -\delta_{ij}\frac{\alpha}{6\pi}\frac{(\bar{Y}_3^{QL}\bar{Y}_3^{QL\dagger})_{32}}{m_{S_3}^2}\left[\log\left(\frac{m_{S_3}^2}{m_b^2}\right)-\frac{19}{12}\right],
\tag{D4}
$$

$$
\begin{aligned}
[L_{ed}^{V,LL}(m_\tau)]^{\rm NP}_{3222} = & \frac{(\bar{Y}_3^{QL})^*_{23}(\bar{Y}_3^{QL})_{22}}{m_{S_3}^2}\left\{1-\frac{\alpha}{2\pi}\log\left(\frac{m_{S_3}^2}{m_\tau^2}\right)+\frac{g^2(1-4c_W^4)}{32\pi^2c_W^2}\left[\log\left(\frac{m_{S_3}^2}{m_Z^2}\right)+\frac{11}{6}\right]\right\} \\
& +\frac{y_t^2}{64\pi^2}\left\{2V_{ts}^*V_{ts}\frac{(Y_3^{QL})^*_{33}(Y_3^{QL})_{32}}{m_{S_3}^2}+\left[V_{ts}^*\frac{(Y_3^{QL})^*_{33}(\bar{Y}_3^{QL})_{22}}{m_{S_3}^2}+V_{ts}\frac{(\bar{Y}_3^{QL})^*_{23}(Y_3^{QL})_{32}}{m_{S_3}^2}\right]I_{ed}(x_t)\right\} \\
& -\frac{3(N_c+1)}{8}\left[\frac{(\bar{Y}_3^{QL\dagger}\bar{Y}_3^{QL}\bar{Y}_3^{QL\dagger})_{32}(\bar{Y}_3^{QL})_{22}}{(4\pi)^2m_{S_3}^2}+\frac{(\bar{Y}_3^{QL})^*_{23}(\bar{Y}_3^{QL}\bar{Y}_3^{QL\dagger}\bar{Y}_3^{QL})_{22}}{(4\pi)^2m_{S_3}^2}\right] \\
& -\frac{5}{4}\frac{(\bar{Y}_3^{QL\dagger}\bar{Y}_3^{QL})_{32}(\bar{Y}_3^{QL}\bar{Y}_3^{QL\dagger})_{22}}{(4\pi)^2m_{S_3}^2}-\frac{\alpha}{6\pi}N_cQ_d^2\left[\frac{(Y_3^{QL})^*_{33}(Y_3^{QL})_{32}}{m_{S_3}^2}\log\left(\frac{m_t^2}{m_b^2}\right)-\frac{3}{4}\frac{(Y_3^{QL\dagger}Y_3^{QL})_{32}}{m_{S_3}^2}\right] \\
& -N_c(I_{d_L}^3-Q_ds_W^2)y_t^2\frac{(Y_3^{QL})^*_{33}(Y_3^{QL})_{32}}{(4\pi)^2m_{S_3}^2}\left[\log\left(\frac{m_{S_3}^2}{m_t^2}\right)-1\right],
\end{aligned}
\tag{D5}
$$

$$
\begin{aligned}
[L_{ed}^{V,LR}(m_\tau)]^{\rm NP}_{3222} = & -\frac{\alpha}{6\pi}N_cQ_d^2\left[\frac{(Y_3^{QL})^*_{33}(Y_3^{QL})_{32}}{m_{S_3}^2}\log\left(\frac{m_t^2}{m_b^2}\right)-\frac{3}{4}\frac{(Y_3^{QL\dagger}Y_3^{QL})_{32}}{m_{S_3}^2}\right] \\
& -N_c(-Q_ds_W^2)y_t^2\frac{(Y_3^{QL})^*_{33}(Y_3^{QL})_{32}}{(4\pi)^2m_{S_3}^2}\left[\log\left(\frac{m_{S_3}^2}{m_t^2}\right)-1\right],
\end{aligned}
\tag{D6}
$$

$$
\begin{aligned}
[L_{ee}^{V,LL}(m_\tau)]_{3222} = & -\frac{5N_c}{8}\frac{(Y_3^{QL\dagger}Y_3^{QL})_{32}(Y_3^{QL\dagger}Y_3^{QL})_{22}}{(4\pi)^2m_{S_3}^2} \\
& -\frac{\alpha}{12\pi}N_cQ_dQ_e\left[\frac{(Y_3^{QL})^*_{33}(Y_3^{QL})_{32}}{m_{S_3}^2}\log\left(\frac{m_t^2}{m_b^2}\right)-\frac{3}{4}\frac{(Y_3^{QL\dagger}Y_3^{QL})_{32}}{m_{S_3}^2}\right] \\
& -\frac{N_c}{2}(I_{e_L}^3-Q_es_W^2)y_t^2\frac{(Y_3^{QL})^*_{33}(Y_3^{QL})_{32}}{(4\pi)^2m_{S_3}^2}\left[\log\left(\frac{m_{S_3}^2}{m_t^2}\right)-1\right],
\end{aligned}
\tag{D7}
$$

$$
\begin{aligned}
[L_{ee}^{V,LR}(m_\tau)]_{3222} = & -\frac{\alpha}{6\pi}N_cQ_dQ_e\left[\frac{(Y_3^{QL})^*_{33}(Y_3^{QL})_{32}}{m_{S_3}^2}\log\left(\frac{m_t^2}{m_b^2}\right)-\frac{3}{4}\frac{(Y_3^{QL\dagger}Y_3^{QL})_{32}}{m_{S_3}^2}\right] \\
& -N_c(-Q_es_W^2)y_t^2\frac{(Y_3^{QL})^*_{33}(Y_3^{QL})_{32}}{(4\pi)^2m_{S_3}^2}\left[\log\left(\frac{m_{S_3}^2}{m_t^2}\right)-1\right],
\end{aligned}
\tag{D8}
$$

$$
[L_{e\gamma}(m_\tau)]^{\rm NP}_{ij} = \frac{eN_cm_{e_j}}{8}\frac{(Y_3^{QL\dagger}Y_3^{QL})_{ij}}{(4\pi)^2m_{S_3}^2},
\tag{D9}
$$

$$[L_{dd}^{V,LL}(m_b)]_{2323}^{\rm NP} = -\frac{5}{8}\frac{(\bar{Y}_3^{QL}\bar{Y}_3^{QL\dagger})_{32}(\bar{Y}_3^{QL}\bar{Y}_3^{QL\dagger})_{32}}{(4\pi)^2 m_{S_3}^2}, \quad \text{(D10)}$$

where $Q_d = -1/3$, $Q_e = -1$, $I_{d_L}^3 = I_{e_L}^3 = -1/2$, and $I_{\nu d}(x)$ is the loop function defined by

$$I_{\nu d}(x) = -\log\left(\frac{m_{S_3}^2}{m_W^2}\right) - \frac{3(x+1)}{2(x-1)} + \frac{x^2+10x-8}{(x-1)^2}\log x. \quad \text{(D11)}$$

Similar one-loop expressions for the low-energy coefficients can also be found in Refs. [138–141].

APPENDIX E: $Z \to \mu^\mp\tau^\pm$

The S_3 affects the Z-boson effective couplings with charged leptons which are defined as

$$\mathcal{L} = \frac{e}{s_W c_W} Z_\mu [\bar{e}_{Li}\gamma_\mu (g_L^e)_{ij} e_{Lj} + \bar{e}_{Ri}\gamma_\mu (g_R^e)_{ij} e_{Rj}], \quad \text{(E1)}$$

where $(g_L^e)_{ij} = g_L^{e,\rm SM}\delta_{ij} + (g_L^e)_{ij}^{\rm NP}$ and $(g_R^e)_{ij} = g_R^{e,\rm SM}\delta_{ij} + (g_R^e)_{ij}^{\rm NP}$ with the SM tree-level couplings $g_L^{e,\rm SM} = I_{e_L}^3 - Q_e s_W^2$ and $g_R^{e,\rm SM} = -Q_e s_W^2$. According to Ref. [126] (see also Refs. [141–143]), the S_3 contribution to the left-handed coupling reads as

$$\begin{aligned}(g_L^e)_{ij}^{\rm NP} = {} & \frac{N_c}{(4\pi)^2}\left[(g_L^{u,\rm SM} - g_R^{u,\rm SM})\frac{x_t(x_t - 1 - \log x_t)}{(x_t-1)^2} + \frac{x_Z}{12}F(x_t) + \mathcal{O}(x_Z^2)\right](Y_3^{QL*})_{3i}(Y_3^{QL})_{3j} \\ & + \frac{N_c x_Z}{3(4\pi)^2}\left[g_L^{u,\rm SM}\left(\log x_Z - i\pi - \frac{1}{6}\right) + \frac{g_L^{e,\rm SM}}{6}\right]\sum_{w=1}^{2}(Y_3^{QL*})_{wi}(Y_3^{QL})_{wj} \\ & + \frac{2N_c x_Z}{3(4\pi)^2}\left[g_L^{d,\rm SM}\left(\log x_Z - i\pi - \frac{1}{6}\right) + \frac{g_L^{e,\rm SM}}{6}\right]\sum_{w=1}^{3}(\bar{Y}_3^{QL*})_{wi}(\bar{Y}_3^{QL})_{wj}, \end{aligned} \quad \text{(E2)}$$

where $x_Z = m_Z^2/m_{S_3}^2$, $x_t = m_t^2/m_{S_3}^2$, $g_L^{u,\rm SM}$, $g_R^{u,\rm SM}$ and $g_L^{d,\rm SM}$ are the SM couplings for up-type and down-type quarks defined analogous to those for charged leptons, and the function $F(x)$ is defined as

$$\begin{aligned}F(x) = {} & -g_L^{u,\rm SM}\frac{(x-1)(5x^2-7x+8) - 2(x^3+2)\log x}{(x-1)^4} - g_R^{u,\rm SM}\frac{(x-1)(x^2-5x-2)+6x\log x}{(x-1)^4} \\ & + g_L^{e,\rm SM}\frac{(x-1)(-11x^2+7x-2)+6x^3\log x}{3(x-1)^4}. \end{aligned} \quad \text{(E3)}$$

Using the above effective coupling, the branching ratio for $Z \to \mu^\mp\tau^\pm$ is given by

$$\mathcal{B}(Z\to\mu^\mp\tau^\pm) = \mathcal{B}(Z\to\mu^-\tau^+) + \mathcal{B}(Z\to\mu^+\tau^-) = \frac{G_F m_Z^3}{3\pi\sqrt{2}\Gamma_Z}(|(g_L^e)_{23}^{\rm NP}|^2 + |(g_L^e)_{32}^{\rm NP}|^2), \quad \text{(E4)}$$

where Γ_Z is the total decay width of Z boson.

[1] J. C. Pati and A. Salam, Phys. Rev. Lett. **31**, 661 (1973).
[2] J. C. Pati and A. Salam, Phys. Rev. D **10**, 275 (1974); **11**, 703(E) (1975).
[3] H. Georgi and S. L. Glashow, Phys. Rev. Lett. **32**, 438 (1974).
[4] H. Georgi, H. R. Quinn, and S. Weinberg, Phys. Rev. Lett. **33**, 451 (1974).
[5] H. Georgi, AIP Conf. Proc. **23**, 575 (1975).
[6] H. Fritzsch and P. Minkowski, Ann. Phys. (N.Y.) **93**, 193 (1975).
[7] P. Langacker, Phys. Rep. **72**, 185 (1981).
[8] P. Langacker, in *Prodceedings of the 1st International Symposium on Particles, Strings and Cosmology* (World Scientific, Singapore, 1990), pp. 237–269.
[9] J. R. Ellis, S. Kelley, and D. V. Nanopoulos, Phys. Lett. B **260**, 131 (1991).
[10] U. Amaldi, W. de Boer, and H. Furstenau, Phys. Lett. B **260**, 447 (1991).
[11] P. Langacker and M.-x. Luo, Phys. Rev. D **44**, 817 (1991).
[12] C. Giunti, C. W. Kim, and U. W. Lee, Mod. Phys. Lett. A **06**, 1745 (1991).
[13] K. S. Babu and E. Ma, Phys. Lett. **144B**, 381 (1984).

[14] H. Murayama and T. Yanagida, Mod. Phys. Lett. A **07**, 147 (1992).
[15] A. Giveon, L. J. Hall, and U. Sarid, Phys. Lett. B **271**, 138 (1991).
[16] I. Dorsner and P. Fileviez Perez, Nucl. Phys. **B723**, 53 (2005).
[17] I. Dorsner, P. Fileviez Perez, and R. Gonzalez Felipe, Nucl. Phys. B**747**, 312 (2006).
[18] I. Dorsner and P. Fileviez Perez, Phys. Lett. B **642**, 248 (2006).
[19] I. Dorsner, P. Fileviez Perez, and G. Rodrigo, Phys. Rev. D **75**, 125007 (2007).
[20] B. Bajc and G. Senjanovic, J. High Energy Phys. 08 (2007) 014.
[21] P. Fileviez Perez, Phys. Lett. B **654**, 189 (2007).
[22] I. Dorsner and I. Mocioiu, Nucl. Phys. **B796**, 123 (2008).
[23] P. Fileviez Perez, H. Iminniyaz, and G. Rodrigo, Phys. Rev. D **78**, 015013 (2008).
[24] I. Dorsner, S. Fajfer, J. F. Kamenik, and N. Kosnik, Phys. Rev. D **81**, 055009 (2010).
[25] P. Fileviez Perez and C. Murgui, Phys. Rev. D **94**, 075014 (2016).
[26] P. Cox, A. Kusenko, O. Sumensari, and T. T. Yanagida, J. High Energy Phys. 03 (2017) 035.
[27] I. Doršner, S. Fajfer, and N. Košnik, Eur. Phys. J. C **77**, 417 (2017).
[28] D. Bečirević, I. Doršner, S. Fajfer, D. A. Faroughy, N. Košnik, and O. Sumensari, Phys. Rev. D **98**, 055003 (2018).
[29] J. Schwichtenberg, Eur. Phys. J. C **79**, 351 (2019).
[30] N. Haba, Y. Mimura, and T. Yamada, Phys. Rev. D **99**, 075018 (2019).
[31] H. Georgi and C. Jarlskog, Phys. Lett. **86B**, 297 (1979).
[32] M. H. Rahat, P. Ramond, and B. Xu, Phys. Rev. D **98**, 055030 (2018).
[33] M. J. Pérez, M. H. Rahat, P. Ramond, A. J. Stuart, and B. Xu, Phys. Rev. D **100**, 075008 (2019).
[34] M. J. Pérez, M. H. Rahat, P. Ramond, A. J. Stuart, and B. Xu, Phys. Rev. D **101**, 075018 (2020).
[35] W. Buchmuller, R. Ruckl, and D. Wyler, Phys. Lett. B **191**, 442 (1987); **448**, 320(E) (1999).
[36] I. Doršner, S. Fajfer, A. Greljo, J. F. Kamenik, and N. Košnik, Phys. Rep. **641**, 1 (2016).
[37] Y. Sakaki, R. Watanabe, M. Tanaka, and A. Tayduganov, Phys. Rev. D **88**, 094012 (2013).
[38] G. Hiller and M. Schmaltz, Phys. Rev. D **90**, 054014 (2014).
[39] A. K. Alok, B. Bhattacharya, D. Kumar, J. Kumar, D. London, and S. U. Sankar, Phys. Rev. D **96**, 015034 (2017).
[40] I. Doršner, S. Fajfer, D. A. Faroughy, and N. Košnik, J. High Energy Phys. 10 (2017) 188.
[41] L. Di Luzio, M. Kirk, and A. Lenz, Phys. Rev. D **97**, 095035 (2018).
[42] S. Fajfer, N. Košnik, and L. Vale Silva, Eur. Phys. J. C **78**, 275 (2018).
[43] J. Alda, J. Guasch, and S. Penaranda, Eur. Phys. J. C **79**, 588 (2019).
[44] R. Mandal and A. Pich, J. High Energy Phys. 12 (2019) 089.
[45] L. Di Luzio, M. Kirk, A. Lenz, and T. Rauh, J. High Energy Phys. 12 (2019) 009.
[46] A. Angelescu, D. Bečirević, D. A. Faroughy, F. Jaffredo, and O. Sumensari, Phys. Rev. D **104**, 055017 (2021).
[47] A. Crivellin, D. Müller, and L. Schnell, Phys. Rev. D **103**, 115023 (2021); **104**, 055020(A) (2021).
[48] N. Košnik and A. Smolkovič, Phys. Rev. D **104**, 115004 (2021).
[49] L.-L. Chau and W.-Y. Keung, Phys. Rev. Lett. **53**, 1802 (1984).
[50] P. A. Zyla *et al.* (Particle Data Group), Prog. Theor. Exp. Phys. **2020**, 083C01 (2020).
[51] J. Hisano, H. Murayama, and T. Yanagida, Nucl. Phys. **B402**, 46 (1993).
[52] H. Arason, D. J. Castano, B. Kesthelyi, S. Mikaelian, E. J. Piard, P. Ramond, and B. D. Wright, Phys. Rev. D **46**, 3945 (1992).
[53] P. Nath and P. Fileviez Perez, Phys. Rep. **441**, 191 (2007).
[54] A. Takenaka *et al.* (Super-Kamiokande Collaboration), Phys. Rev. D **102**, 112011 (2020).
[55] K. G. Chetyrkin, J. H. Kuhn, and M. Steinhauser, Comput. Phys. Commun. **133**, 43 (2000).
[56] F. Herren and M. Steinhauser, Comput. Phys. Commun. **224**, 333 (2018).
[57] A. Juste Rozas (on behalf of the ATLAS and CMS Collaborations), Report No. ATL-PHYS-SLIDE-2023-034, 2023.
[58] J. de Blas, M. Chala, M. Perez-Victoria, and J. Santiago, J. High Energy Phys. 04 (2015) 078.
[59] J. de Blas, J. Criado, M. Perez-Victoria, and J. Santiago, J. High Energy Phys. 03 (2018) 109.
[60] V. Gherardi, D. Marzocca, and E. Venturini, J. High Energy Phys. 07 (2020) 225; 01 (2021) 006.
[61] E. E. Jenkins, A. V. Manohar, and M. Trott, J. High Energy Phys. 10 (2013) 087.
[62] E. E. Jenkins, A. V. Manohar, and M. Trott, J. High Energy Phys. 01 (2014) 035.
[63] R. Alonso, E. E. Jenkins, A. V. Manohar, and M. Trott, J. High Energy Phys. 04 (2014) 159.
[64] B. Grzadkowski, M. Iskrzynski, M. Misiak, and J. Rosiek, J. High Energy Phys. 10 (2010) 085.
[65] E. E. Jenkins, A. V. Manohar, and P. Stoffer, J. High Energy Phys. 03 (2018) 016.
[66] J. Aebischer, A. Crivellin, M. Fael, and C. Greub, J. High Energy Phys. 05 (2016) 037.
[67] W. Dekens and P. Stoffer, J. High Energy Phys. 10 (2019) 197.
[68] J. Aebischer, M. Fael, C. Greub, and J. Virto, J. High Energy Phys. 09 (2017) 158.
[69] E. E. Jenkins, A. V. Manohar, and P. Stoffer, J. High Energy Phys. 01 (2018) 084.
[70] G. Buchalla, A. J. Buras, and M. E. Lautenbacher, Rev. Mod. Phys. **68**, 1125 (1996).
[71] N. Gubernari, M. Reboud, D. van Dyk, and J. Virto, J. High Energy Phys. 09 (2022) 133.
[72] S. Jäger and J. Martin Camalich, J. High Energy Phys. 05 (2013) 043.
[73] J. Lyon and R. Zwicky, arXiv:1406.0566.
[74] S. Descotes-Genon, L. Hofer, J. Matias, and J. Virto, J. High Energy Phys. 12 (2014) 125.

[75] S. Jäger and J. Martin Camalich, Phys. Rev. D **93**, 014028 (2016).
[76] M. Ciuchini, M. Fedele, E. Franco, S. Mishima, A. Paul, L. Silvestrini, and M. Valli, J. High Energy Phys. 06 (2016) 116.
[77] M. Ciuchini, M. Fedele, E. Franco, A. Paul, L. Silvestrini, and M. Valli, Phys. Rev. D **107**, 055036 (2023).
[78] LHCb Collaboration, Phys. Rev. Lett. **131**, 051803 (2023).
[79] LHCb Collaboration, Phys. Rev. D **108**, 032002 (2023).
[80] R. Aaij *et al.* (LHCb Collaboration), arXiv:1808.08865.
[81] R. L. Workman *et al.* (Particle Data Group), Prog. Theor. Exp. Phys. **2022**, 083C01 (2022).
[82] J. P. Lees *et al.* (*BABAR* Collaboration), Phys. Rev. D **87**, 112005 (2013).
[83] W. Altmannshofer *et al.* (Belle-II Collaboration), Prog. Theor. Exp. Phys. **2019**, 123C01 (2019); **2020**, 029201(E) (2020).
[84] J. Grygier *et al.* (Belle Collaboration), Phys. Rev. D **96**, 091101 (2017); **97**, 099902(E) (2018).
[85] O. Lutz *et al.* (Belle Collaboration), Phys. Rev. D **87**, 111103 (2013).
[86] Y. S. Amhis *et al.* (Heavy Flavor Averaging Group), Phys. Rev. D **107**, 052008 (2023).
[87] R. Aaij *et al.* (LHCb Collaboration), Phys. Rev. Lett. **118**, 251802 (2017).
[88] J. Lees *et al.* (*BABAR* Collaboration), Phys. Rev. Lett. **118**, 031802 (2017).
[89] T. V. Dong *et al.* (Belle Collaboration), Phys. Rev. D **108**, L011102 (2023).
[90] L. Aggarwal *et al.* (Belle-II Collaboration), arXiv:2207.06307.
[91] R. Aaij *et al.* (LHCb Collaboration), Phys. Rev. Lett. **123**, 211801 (2019).
[92] S. Watanuki *et al.* (Belle Collaboration), Phys. Rev. Lett. **130**, 261802 (2023).
[93] R. Aaij *et al.* (LHCb Collaboration), J. High Energy Phys. 06 (2023) 143.
[94] N. Tsuzuki *et al.* (Belle Collaboration), J. High Energy Phys. 06 (2023) 118.
[95] S. Banerjee *et al.* arXiv:2203.14919.
[96] S. Patra *et al.* (Belle Collaboration), J. High Energy Phys. 05 (2022) 095.
[97] J. P. Lees *et al.* (*BABAR* Collaboration), Phys. Rev. Lett. **104**, 151802 (2010).
[98] A. Abdesselam *et al.* (Belle Collaboration), J. High Energy Phys. 10 (2021) 19.
[99] K. Hayasaka *et al.*, Phys. Lett. B **687**, 139 (2010).
[100] G. Aad *et al.* (ATLAS Collaboration), Phys. Rev. Lett. **127**, 271801 (2022).
[101] M. Dam, SciPost Phys. Proc. **1**, 041 (2019).
[102] A. J. Buras, J. Girrbach-Noe, C. Niehoff, and D. M. Straub, J. High Energy Phys. 02 (2015) 184.
[103] E. Ganiev (Belle-II Collaboration), *Proceedings of the European Physical Society Conference on High Energy Physics (EPS-HEP), Hamburg, 2023*.
[104] A. Celis, J. Fuentes-Martin, A. Vicente, and J. Virto, Phys. Rev. D **96**, 035026 (2017).
[105] B. Capdevila, S. Descotes-Genon, L. Hofer, and J. Matias, J. High Energy Phys. 04 (2017) 016.
[106] M. Bordone, G. Isidori, and A. Pattori, Eur. Phys. J. C **76**, 440 (2016).
[107] G. Isidori, S. Nabeebaccus, and R. Zwicky, J. High Energy Phys. 12 (2020) 104.
[108] C. Bobeth, M. Gorbahn, T. Hermann, M. Misiak, E. Stamou, and M. Steinhauser, Phys. Rev. Lett. **112**, 101801 (2014).
[109] T. Blake, G. Lanfranchi, and D. M. Straub, Prog. Part. Nucl. Phys. **92**, 50 (2017).
[110] K. De Bruyn, R. Fleischer, R. Knegjens, P. Koppenburg, M. Merk, and N. Tuning, Phys. Rev. D **86**, 014027 (2012).
[111] K. De Bruyn, R. Fleischer, R. Knegjens, P. Koppenburg, M. Merk, A. Pellegrino, and N. Tuning, Phys. Rev. Lett. **109**, 041801 (2012).
[112] A. Crivellin, D. Müller, and T. Ota, J. High Energy Phys. 09 (2017) 040.
[113] D. Buttazzo, A. Greljo, G. Isidori, and D. Marzocca, J. High Energy Phys. 11 (2017) 044.
[114] C. Bobeth and U. Haisch, Acta Phys. Pol. B **44**, 127 (2013).
[115] B. Capdevila, A. Crivellin, S. Descotes-Genon, L. Hofer, and J. Matias, Phys. Rev. Lett. **120**, 181802 (2018).
[116] A. Dedes, J. Rosiek, and P. Tanedo, Phys. Rev. D **79**, 055006 (2009).
[117] D. Bečirević, O. Sumensari, and R. Zukanovich Funchal, Eur. Phys. J. C **76**, 134 (2016).
[118] A. Abada, D. Bečirević, M. Lucente, and O. Sumensari, Phys. Rev. D **91**, 113013 (2015).
[119] D. E. Hazard and A. A. Petrov, Phys. Rev. D **94**, 074023 (2016).
[120] L. Calibbi, T. Li, X. Marcano, and M. A. Schmidt, Phys. Rev. D **106**, 115039 (2022).
[121] T. Goto, Y. Okada, and Y. Yamamoto, Phys. Rev. D **83**, 053011 (2011).
[122] Y. Okada, K.-i. Okumura, and Y. Shimizu, Phys. Rev. D **61**, 094001 (2000).
[123] Y. Kuno and Y. Okada, Rev. Mod. Phys. **73**, 151 (2001).
[124] T. Aoyama *et al.*, Phys. Rept. **887**, 1 (2020).
[125] D. P. Aguillard *et al.* (Muon g-2 Collaboration), arXiv:2308.06230.
[126] P. Arnan, D. Becirevic, F. Mescia, and O. Sumensari, J. High Energy Phys. 02 (2019) 109.
[127] P. Abreu *et al.* (DELPHI Collaboration), Z. Phys. C **73**, 243 (1997).
[128] A. J. Buras, J. R. Ellis, M. K. Gaillard, and D. V. Nanopoulos, Nucl. Phys. **B135**, 66 (1978).
[129] P. H. Frampton, S. Nandi, and J. J. G. Scanio, Phys. Lett. **85B**, 225 (1979).
[130] P. Kalyniak and J. N. Ng, Phys. Rev. D **26**, 890 (1982).
[131] P. Eckert, J. M. Gerard, H. Ruegg, and T. Schucker, Phys. Lett. **125B**, 385 (1983).
[132] M. E. Machacek and M. T. Vaughn, Nucl. Phys. **B222**, 83 (1983).
[133] M. E. Machacek and M. T. Vaughn, Nucl. Phys. **B236**, 221 (1984).
[134] M. E. Machacek and M. T. Vaughn, Nucl. Phys. **B249**, 70 (1985).
[135] M.-x. Luo, H.-w. Wang, and Y. Xiao, Phys. Rev. D **67**, 065019 (2003).

[136] K. Kowalska, E. M. Sessolo, and Y. Yamamoto, Eur. Phys. J. C **81**, 272 (2021).
[137] M. Fedele, F. Wuest, and U. Nierste, arXiv:2307.15117.
[138] A. Crivellin, D. Müller, and F. Saturnino, J. High Energy Phys. 06 (2020) 020.
[139] V. Gherardi, D. Marzocca, and E. Venturini, J. High Energy Phys. 01 (2021) 138.
[140] M. Bordone, O. Catà, T. Feldmann, and R. Mandal, J. High Energy Phys. 03 (2021) 122.
[141] A. Crivellin, C. Greub, D. Müller, and F. Saturnino, J. High Energy Phys. 02 (2021) 182.
[142] F. Feruglio, P. Paradisi, and A. Pattori, Phys. Rev. Lett. **118**, 011801 (2017).
[143] F. Feruglio, P. Paradisi, and A. Pattori, J. High Energy Phys. 09 (2017) 061.